Great Artery and Other Vascular Abnormalities

13

Wanda C. Miller-Hance

Abstract

Echocardiography is the diagnostic modality of choice in the initial evaluation and serial assessment of most types of pediatric heart disease. The anomalies of a congenital nature that most often affect the great arteries and related vascular structures are frequently first suspected and identified by high-resolution imaging provided by transthoracic echocardiography. Technological advances made during the last several decades allow for complementary noninvasive imaging modalities to be applied when further characterization of these congenital cardiovascular malformations or variants is required. Transesophageal echocardiography (TEE) plays a limited diagnostic role in these anomalies but nonetheless provides major contributions in the care of affected patients. In the intraoperative setting, TEE is able to confirm the presence of selected abnormal vascular structure(s) or connection(s). More importantly, TEE facilitates the detailed evaluation of associated defects, provides for intraoperative monitoring, and allows for assessment of the surgical intervention(s). This chapter discusses the most frequently encountered great artery and vascular anomalies of a congenital nature, focusing on the applications of TEE in the evaluation of these lesions.

Keywords

Great artery anomalies • Vascular anomalies • Patent ductus arteriosus • Aortopulmonary window • Pulmonary artery anomalies • Anomalous origin of a branch pulmonary artery from the aorta • Pulmonary artery sling • Anomalous origin of the left pulmonary artery from the right pulmonary artery • Aortic arch anomalies • Coarctation of the aorta • Interrupted aortic arch

Introduction

In congenital heart disease (CHD), abnormalities of the great arteries and related vascular connections are commonly encountered. Transthoracic echocardiography (TTE) serves as the initial and primary diagnostic tool for their identification and assessment, particularly in the pediatric population. Additional complementary and noninvasive imaging modalities, such as cardiac magnetic resonance imaging (MRI) and computerized tomography (CT), can also be used to characterize these pathologies further, while at the same time providing information regarding related intracardiac and extracardiac structures.

In most, if not all, cases, TTE alone or in combination with these other imaging studies is able to define fully the abnormalities that affect the great arteries and delineate abnormal vascular connections. Thus, transesophageal echocardiography (TEE) generally does not play a major diagnostic role in these malformations. However despite certain challenges, the assessment of the great arteries and vascular

W.C. Miller-Hance, MD, FACC, FASE
Divisions of Pediatric Anesthesiology and Pediatric Cardiology,
Departments of Pediatrics and Anesthesiology,
Texas Children's Hospital, Baylor College of Medicine,
6621 Fannin, Suite W17417, Houston, TX 77030, USA
e-mail: wmh@bcm.edu

The online version of this chapter (doi:10.1007/978-1-84800-064-3_13) contains supplementary material, which is available to authorized users.

P.C. Wong, W.C. Miller-Hance (eds.), *Transesophageal Echocardiography for Congenital Heart Disease*,
DOI 10.1007/978-1-84800-064-3_13,

anomalies is feasible by TEE. In the operating room setting, in addition to providing confirmation of the abnormalities affecting these structures, TEE allows for evaluation of associated pathology, exclusion of suspected defects, and intraoperative monitoring. TEE can also provide a method for the assessment of an intervention or surgical procedure affecting the great arteries or related vascular structures; at the same time it serves a very important role in determining the adequacy of repair of any coexisting lesion(s). In this setting, TEE functions to identify and correct (or at least limit) residual pathology of hemodynamic significance that might negatively impact patient outcome.

This chapter addresses selected malformations that primarily affect the great arteries and highlights the most commonly found abnormal connections between these vascular structures. The discussion focuses on the role of TEE in the assessment of these anomalies with an emphasis on perioperative applications. As an introduction to the subject, the reader is referred to Chap. 4 for a detailed discussion of TEE imaging of the great arteries. The overview presented there should serve as a foundation for this chapter and will facilitate understanding of the lesions/variants discussed. Anomalies of venous structures are presented in Chap. 6 and will not be addressed here.

Abnormal Vascular Connections

Patent Ductus Arteriosus

Anatomic Features

The ductus arteriosus is a vascular channel that connects the pulmonary trunk to the proximal descending aorta. Anatomically, the ductus arteriosus typically originates from the posterosuperior aspect of the junction between the main and left pulmonary artery, and inserts into the anterolateral or ventral aspect of the descending thoracic aorta, just distal to the origin of the left subclavian artery (Fig. 13.1). Among individuals, the ductus arteriosus may vary in its position, course, size, and length.

In most patients with a left aortic arch, the ductus arteriosus is a left-sided structure. A right or left-sided ductus may be present in patients with a right aortic arch. In some cases, the ductus arteriosus originates from the innominate or subclavian arteries or may even be duplicated (bilateral ductus). Two important issues merit mention: (1) anatomic factors such as aortic arch sidedness, aortic arch branching pattern, and ductal origin/position may result in anomalies causing a vascular ring [1] and (2) an abnormal location, course or shape of the ductus arteriosus, as well as bilateral ductus, are more likely to occur in the setting of complex CHD.

In the normal fetal circulation, the right ventricle generates approximately two-thirds of the fetal cardiac output.

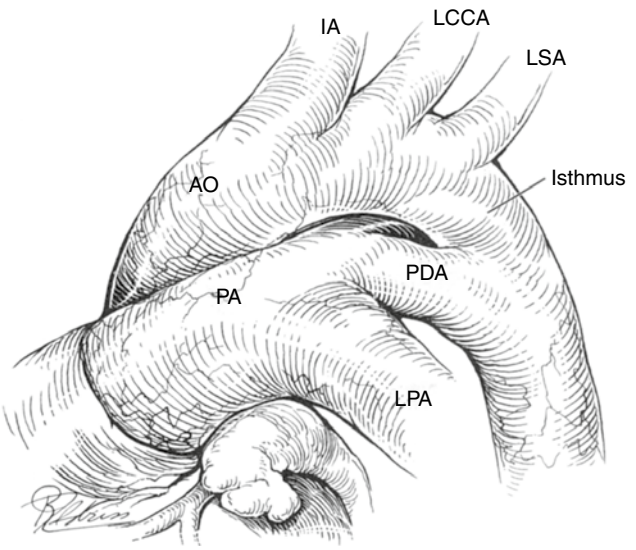

Fig. 13.1 Patent ductus arteriosus. Graphic depiction of patent ductus arteriosus (*PDA*) as visualized from a left anterior oblique view. The typical ductus extends as illustrated from the junction of the main pulmonary artery (*PA*) with the left pulmonary artery (*LPA*) to the descending thoracic aorta just distal to the left subclavian artery (*LSA*). *AO* aorta, *IA* innominate artery, *LCCA* left common carotid artery (Reproduced with permission from Hillman et al. [130])

The majority of this blood is ejected into the descending aorta through the ductus arteriosus, as only a small fraction of the right ventricular output (5–10 %) passes through the lungs. Thus, this communication is an essential component of normal fetal life, allowing for right ventricular ejection into the descending aorta within the context of a high-resistance pulmonary circulation.

In the normal full-term infant, functional closure of the ductus arteriosus occurs several hours after birth. Anatomic closure of this channel takes place in the first few weeks of life. Failure of the ductus arteriosus to close, a process not completely understood, results in persistent ductal patency (*patent ductus arteriosus* or PDA). As an isolated lesion, it accounts for between 4 and 12 % of all cases of CHD.

Associated Defects

A PDA can be found in isolation or in association with other cardiovascular anomalies (e.g., atrial septal defect, ventricular septal defect, atrioventricular septal defect, coarctation of the aorta). A high incidence is found in premature neonates, infants with respiratory distress syndrome, patients affected by rubella syndrome, and children living at high altitudes. Ductal-dependency for either pulmonary or systemic blood flow may be part of the physiology of moderate to severe forms of CHD. The discussion that follows focuses primarily on the PDA as an isolated lesion. The presence and role of the PDA in association with other cardiac defects is also briefly addressed.

Pathophysiology

In the isolated PDA, shunt magnitude is determined by the physical size of the communication (length and internal diameter) and the relationship between the systemic and pulmonary vascular resistances. A small PDA may have little to no physiologic impact. However, the hemodynamic effects of moderate-to-large communications are those of a classic left-to-right shunt manifested by increased pulmonary blood flow, resulting in left atrial and left ventricular volume overload. In a moderate size PDA, an element of ductal constriction is present, so shunting is restrictive to some extent and the pulmonary artery pressure is mildly elevated or may even be normal. Large communications are associated with a greater degree of pulmonary artery pressure elevation. In this setting, shunting can be bidirectional and dictated primarily by the resistances of the vascular beds at either sides of the PDA. The increased left atrial pressure associated with large shunts may lead to stretching of the foramen ovale and result in an additional shunt at this level, further compounding the volume load presented to the pulmonary arteries.

Management Considerations

The management options in the infant beyond prematurity or in the older child who requires ductal closure are occlusion of the communication in the cardiac catheterization laboratory or surgical closure. Various approaches have been used for surgical closure of the isolated PDA, including closed procedures via thoracoscopy (either robotically or video assisted) and open interventions, in most cases, via a thoracotomy. The adult or older patient with a PDA presents a challenge as friable tissue, aneurysmal dilation, or ductal calcification increases the likelihood of procedural complications.

Applications of Transesophageal Echocardiography

TEE has been used for diagnostic applications in the detection and characterization of flow across a PDA [2–8]. However, the use of TEE for this sole purpose is relatively rare. As previously noted, a ductus or ligamentum arteriosum may be part of a vascular ring. In these cases transesophageal instrumentation is generally avoided as probe placement or manipulation can lead to airway compromise due to compression of the trachea by surrounding vascular structures.

In the current era, transcatheter interventions aimed at ductal occlusion are guided primarily by fluoroscopy and angiography. Although TEE has been used in this setting [8, 9], and more recently, three-dimensional (3D) TEE has also been applied [10, 11], its role in these procedures is limited. The use of TEE has also been documented during interventions involving thoracoscopic surgery for the PDA, as well as open procedures in both children and adults [12–16]. The primary role is that of evaluation of shunt flow and magnitude, as well as the success of surgery in obliterating the communication. Currently, TEE is not considered an indication solely for monitoring or assessing the results of surgical closure of an isolated PDA. As such, the discussion that follows is relevant mostly to the use of TEE in the evaluation of patients undergoing surgical ligation or division of a PDA in the setting in which additional cardiac defects are also being addressed.

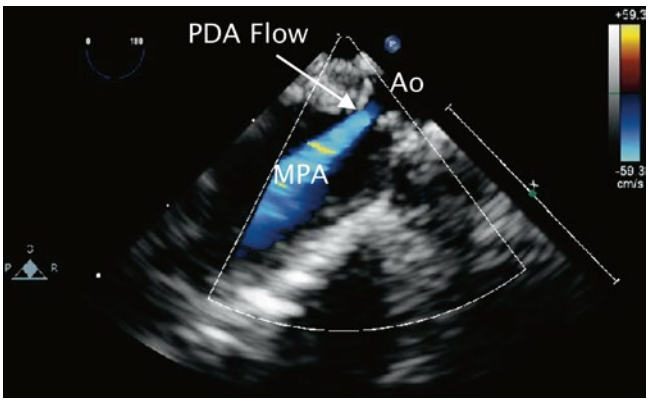

Fig. 13.2 Patent ductus arteriosus. Upper esophageal pulmonary artery long axis view demonstrating flow by color Doppler (*blue signal* away from imaging probe) corresponding to left-to-right shunting across a patent ductus arteriosus (*PDA flow*). *Ao* aorta, *MPA* main pulmonary artery

Goals of TEE Prior to Catheter or Surgical Intervention

Visualization of a PDA and Detection of Ductal Shunting

Direct imaging of the ductus arteriosus to assess patency can be challenging by two-dimensional (2D) transesophageal imaging alone. The examination of a PDA relies to a significant extent on the use of Doppler ultrasound techniques that interrogate flow across the pulmonary artery and descending aorta. The upper esophageal views, particularly the upper esophageal pulmonary artery long axis (UE PA LAX) and the upper esophageal aortic arch short axis (UE Ao Arch SAX), are essential for this evaluation (Fig. 13.2, Video 13.1). These views allow direct visualization of the ductal communication between the aorta and pulmonary artery. In addition, the mid esophageal ascending aortic short axis (ME Asc Ao SAX) with probe anteflexion and counterclockwise rotation, and the mid esophageal right ventricular inflow-outflow (ME RV In-Out) views (Fig. 13.3, Video 13.2), can also provide evidence of left-to-right ductal shunting into the pulmonary artery. As described below, views of the descending aorta that allow for the characterization of flow are also helpful. The combination of these different TEE views for the typical left-sided PDA enables visualization of the communication, including detection of ductal shunting,

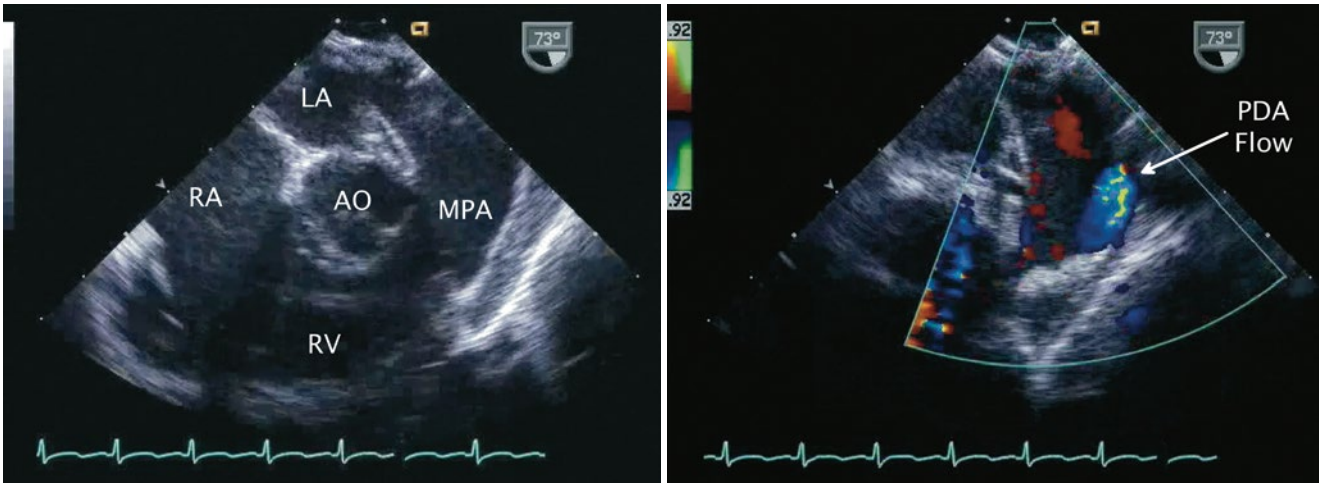

Fig. 13.3 Patent ductus arteriosus. *Left panel*, two-dimensional image of mid esophageal right ventricular inflow-outflow view. *Right panel*, corresponding color Doppler image depicts flow (blue signal) from patent ductus arteriosus (*PDA*) into main pulmonary artery (*MPA*). *AO* aorta, *LA* left atrium, *RA* right atrium, *RV* right ventricle

determination of shunt direction, and gross estimation of shunt magnitude.

Characterization of Flow Across a PDA

In the setting of a restrictive ductus arteriosus and relatively normal pulmonary artery pressures, the higher systemic arterial pressure results in continuous left-to-right shunting into the pulmonary artery throughout the cardiac cycle. This communication can be demonstrated by spectral Doppler assessment and color flow mapping in the upper esophageal, ME Asc Ao SAX, and ME RV In-Out views as previously described. Sampling near the pulmonary end in this case displays continuous high velocity flow, peaking in late systole directed away from the transducer. Color flow Doppler mapping increases the sensitivity of the interrogation and demonstrates turbulent or aliased flow (seen as a mosaic color pattern) from the PDA into the distal main pulmonary artery (Fig. 13.4, Video 13.3). The ductal flow can extend to the level of the pulmonary valve, or beyond into the right ventricular outflow tract, in the presence of pulmonary regurgitation.

In the setting of pulmonary hypertension, shunting across the ductus is continuous and of low velocity, peaking in late systole [17, 18]. As the pulmonary artery pressure and pulmonary vascular resistance increase, there will be blunting of the left-to-right shunt in diastole, so that systolic left-to-right shunting predominates. Further increases in pulmonary artery pressure/vascular resistance result in low velocity bidirectional ductal shunting (right-to-left during systole and left-to-right in late systole extending into late diastole) [19]. This flow pattern can also be seen in ductal-dependent left-sided obstructive lesions such as hypoplastic left heart syndrome or interrupted aortic arch (see below) and can also be a normal

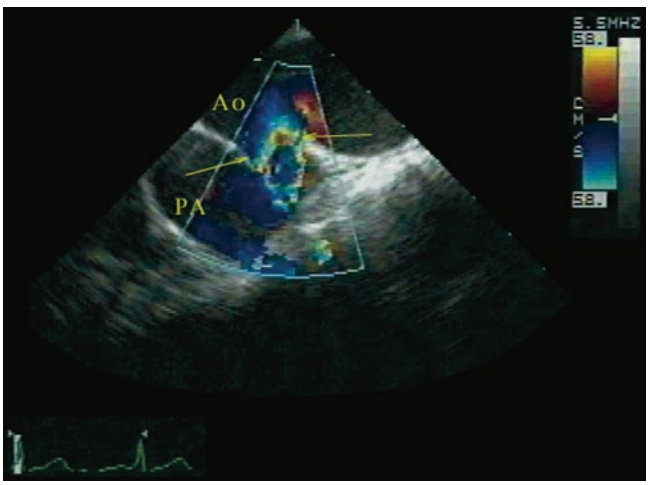

Fig. 13.4 Patent ductus arteriosus. Upper esophageal aortic arch short axis view with color mapping demonstrating aliased flow from the aorta (*Ao*) into the pulmonary artery (*PA*) across a patent ductus arteriosus (*arrows*) (Reproduced with permission from Russell et al. [131])

finding in the neonate [20]. Increasing levels of pulmonary artery pressures and the development of increased pulmonary vascular resistance are characterized by blunting of the left-to-right shunt in diastole. In some cases, exclusive right-to-left ductal shunting is present (reverse ductal shunting), peaking in early systole; this pattern is generally seen with significant elevation in pulmonary artery pressure/vascular resistance (such as obstructed total anomalous pulmonary venous return), and in many cases can be difficult to detect by TEE. Injection of agitated saline into a peripheral or central venous catheter while imaging the descending aorta may demonstrate microcavitations distal to the level of the left subclavian artery, consistent with ductal level right-to left shunting. [6]

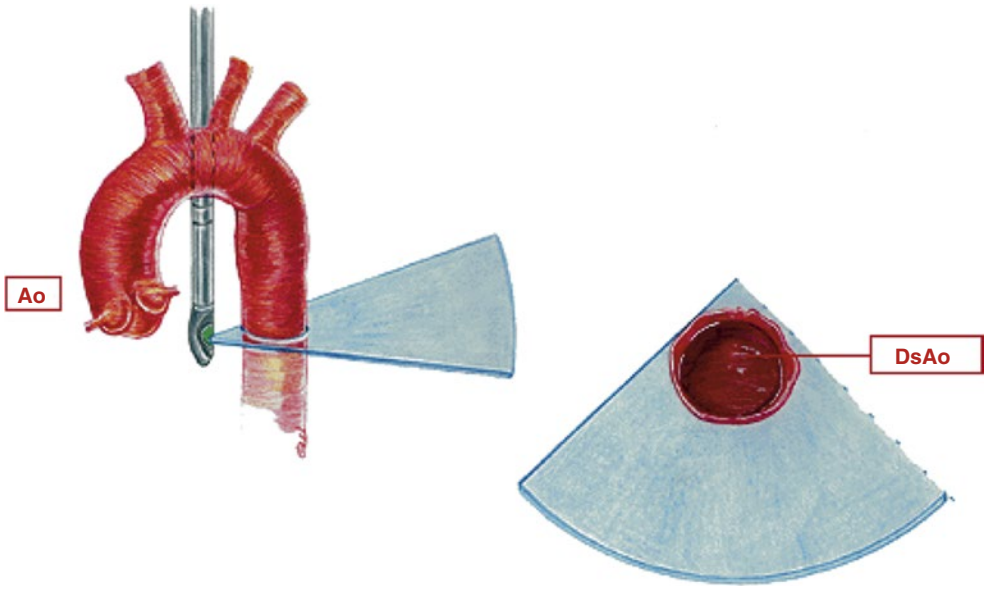

Fig. 13.5 Descending aorta. Graphic illustration of imaging probe position and cross-section displayed in the mid esophageal descending aortic short axis view. *Ao* ascending aorta, *DsAo* descending aorta (Reproduced with permission from Cahalan [132])

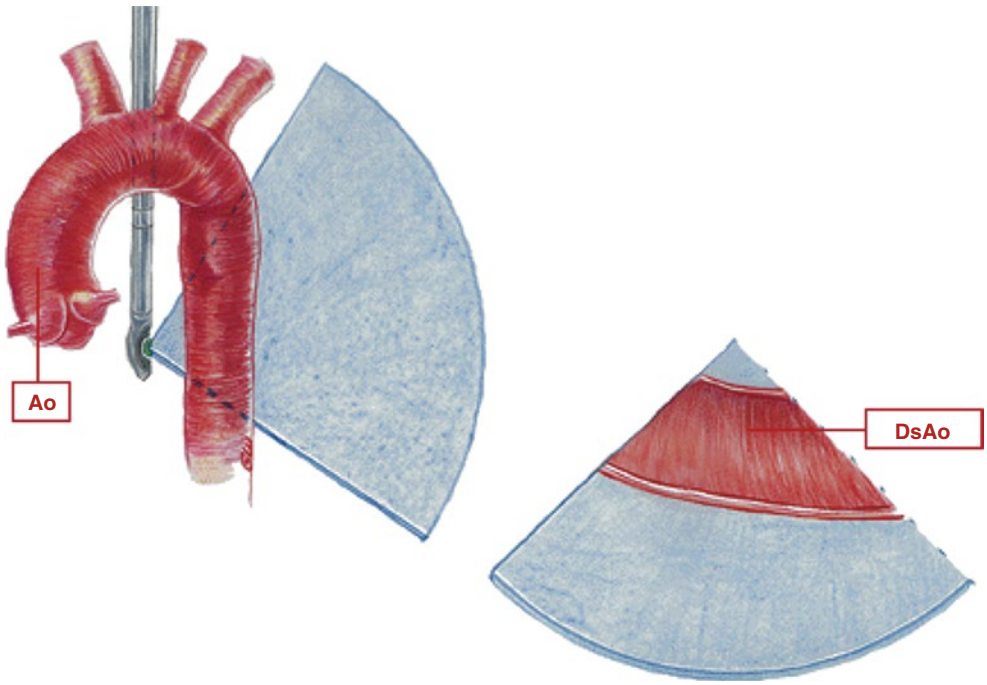

Fig. 13.6 Descending aorta. Graphic illustration of imaging probe position and cross-section displayed in the mid esophageal descending aortic long axis view. *Ao* ascending aorta, *DsAo* descending aorta (Reproduced with permission from Cahalan [132])

Doppler Interrogation of Descending Aorta

The presence of a PDA in association with a large amount of shunt flow may also be suggested by an increase in the caliber of the descending aortic pulsations. Spectral Doppler analysis in the descending aorta demonstrates both antegrade systolic flow and diastolic flow reversal. They are best appreciated in the descending aortic short (Desc Ao SAX, Fig. 13.5) and long axis (Desc Ao LAX, Fig. 13.6) views, in the areas distal to the ductus arteriosus. The retrograde flow represents diastolic runoff into the pulmonary circulation within the context of low pulmonary artery diastolic pressures (Figs. 13.7 and 13.8). The presence and magnitude of holodiastolic flow reversal in the distal descending aorta also provide clues regarding the extent of ductal shunting, as increasing degrees of retrograde flow are present with larger shunts. A parameter that has been examined by transthoracic imaging to estimate shunt size is the ratio of the areas corresponding to retrograde and forward flows [21]. Although not yet validated for TEE, this may also provide a crude index of shunt magnitude.

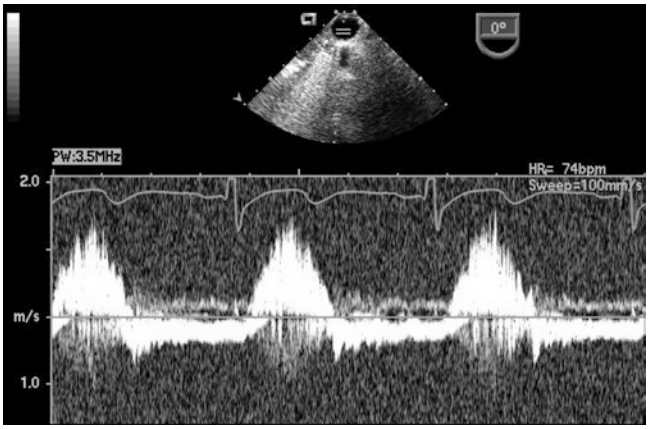

Fig. 13.7 Patent ductus arteriosus. Spectral Doppler interrogation in the mid esophageal descending aortic short axis view demonstrating systolic forward flow as well flow reversal that continues throughout diastole in a patient with a patent ductus arteriosus

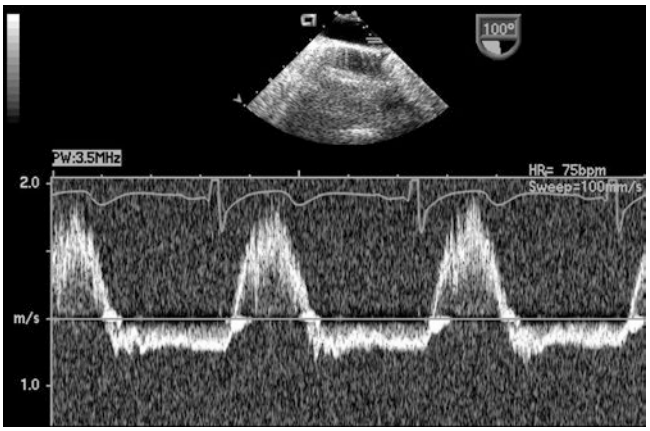

Fig. 13.8 Patent ductus arteriosus. Spectral Doppler tracing obtained by rotating the imaging plane to an orthogonal orientation (mid esophageal descending aorta long axis view) with respect to same patient and probe position as shown in Fig. 13.7. This view provides a more suitable angle for Doppler interrogation and likewise demonstrates holodiastolic flow reversal in the distal descending aorta in association with a patent ductus arteriosus

Estimation of Pulmonary Artery Systolic Pressure from the PDA Jet

The use of Doppler ultrasound facilitates the assessment of systolic pressure gradients between the systemic and pulmonary circulations and estimation of the pulmonary artery systolic pressure (PASP) [22, 23]. This can be accomplished by examining the velocity from the left-to-right jet across the ductus as follows [24]:

$$\mathrm{PASP} = \mathrm{SBP} - 4\mathrm{V}^2$$

V, represents the peak flow velocity (in meters per second) across the ductus in late systole; SBP, systolic blood pressure

Several limitations have been described in the assessment of PASP using this approach [23]. Although they have been reported for transthoracic imaging, these issues are also relevant to TEE. These limitations include potential errors related to position of the spectral sample volume, possible contamination of the continuous wave Doppler signal by flow from adjacent structures, and a PDA shape that does not allow for optimal Doppler cursor alignment for determination of maximal flow velocity, resulting in underestimation of the true pressure drop across the communication. This last issue may be more significant during TEE imaging, as movement of the probe is confined within the esophagus/stomach, in contrast to one's ability to move a transthoracic probe freely across multiple windows to optimize the Doppler evaluation.

Estimation of PASP from the Tricuspid Regurgitant Jet Velocity

Right ventricular systolic pressure (RVSP) also can be estimated from the peak velocity of a tricuspid regurgitant jet, if present (Fig. 13.9, Video 13.4), using the following equation:

$$\mathrm{PASP\ or\ RVSP} = 4\mathrm{V}^2 + \mathrm{RAp}\left(\mathrm{if\ available}\right)$$

V, represents the peak flow velocity of the tricuspid regurgitant jet (in meters/second); RAp, mean right atrial pressure [25].

In the absence of right ventricular outflow tract obstruction, RVSP equals PASP.

Evaluation of Left Atrial and Left Ventricular Size for Dilation

In the absence of co-existing structural defects, the size of the main pulmonary artery, left atrium, and left ventricle may correlate with the degree of the ductal shunting (Fig. 13.10, Video 13.5).

Additional Applications

The assessment of associated cardiovascular defects (e.g., atrioventricular septal defect, subaortic stenosis) represents the main indication for the use of intraoperative TEE in patients with a PDA. The approach suggested in Chap. 4 for the structural evaluation of the heart by TEE should be followed. Depending upon the nature of the associated defects, suitable TEE planes should be obtained to assess the details of the anatomy. Aspects to be examined as part of a comprehensive examination include (but are not limited to) interrogation of atrioventricular and semilunar valves, outflow tracts, and assessment of ventricular systolic function. However even when evaluation of other defects is the primary objective, the mid and upper esophageal TEE views (as noted above) should still be obtained to evaluate the PDA. Of note, it is good practice to utilize these views on a regular basis whenever a comprehensive study is performed; occasionally one can discover a PDA that had previously been unsuspected.

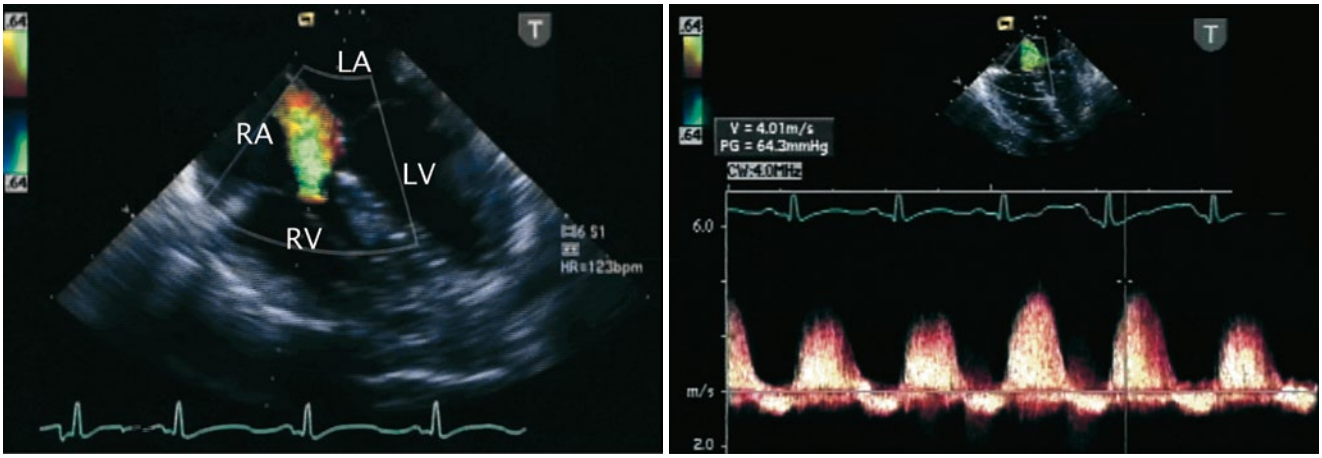

Fig. 13.9 Tricuspid regurgitation. Mid esophageal four chamber view illustrating the jet of tricuspid regurgitation displayed by color flow imaging (*left panel*) and the corresponding spectral Doppler tracing (*right panel*). Note that the peak velocity of the regurgitant jet reaches nearly 4 m/s. The peak velocity predicts an elevated right ventricular and pulmonary artery pressure in this infant. *LA* left atrium, *LV* left ventricle, *RA* right atrium, *RV* right ventricle

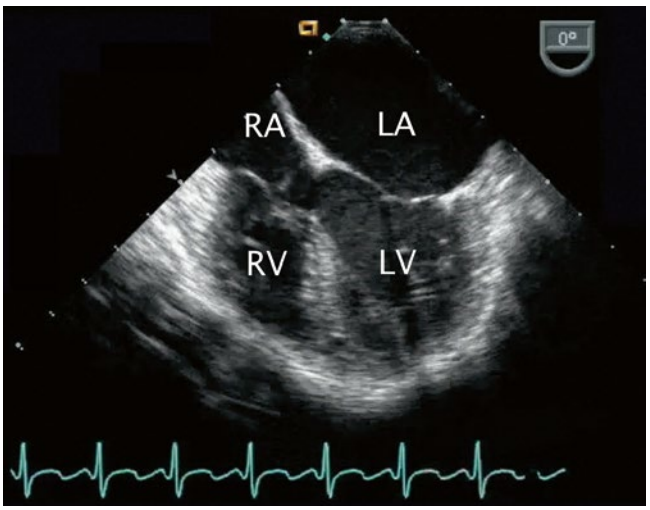

Fig. 13.10 Left heart dilation resulting from a patent ductus arteriosus. Image depicts a mid esophageal four chamber view in a patient with a volume-loaded left heart corresponding to left-to-right ductal level shunting as manifested by dilation of left-sided structures, particularly the left atrium in this case. A tricuspid valve aneurysm is seen. *LA* left atrium, *LV* left ventricle, *RA* right atrium, *RV* right ventricle

Goals of TEE After Catheter or Surgical Intervention

Detection of Residual Ductal Shunting

The magnitude of residual ductal shunting during transcatheter closure or surgery is likely to be relatively small, if at all present. Under these circumstances, a signal representing high velocity, disturbed flow with shunting in the left-to-right direction may be detected in the distal aspect of the main pulmonary artery, near the origin of the left pulmonary artery (in the presence of a left aortic arch).

Additional Applications

Depending on the nature of associated cardiovascular lesions and the catheter-based or surgical intervention(s) performed, TEE should be applied to the post procedure evaluation, as pertinent for the pathology as discussed throughout this textbook.

Aortopulmonary Window

Anatomic Features

Aortopulmonary (AP) window, also referred to as *aortopulmonary septal defect*, *aortopulmonary fenestration*, and *aorticopulmonary window/septal defect*, is a malformation characterized by a defect in the wall between the ascending aorta and the pulmonary artery, creating a communication between these structures [26]. It is thought to be the result of abnormal development of the AP septum. Anatomically and physiologically, an AP window can resemble a truncus arteriosus; however unlike, truncus arteriosus, two distinct semilunar valves are present. It represents a rare defect, accounting for 0.1 % of all congenital cardiovascular anomalies.

The size and location of the communication can vary related to the extent of faulty partitioning of the AP septum. Mori and colleagues classified the AP window into three types (Fig. 13.11) [27]:

- Type I: found in the proximal aspect of the AP septum, located just above the sinuses of Valsalva; it represents the most common type of the defect (referred to as *proximal defect*)
- Type II: found in the most distal part of the AP septum or most superior aspect of the ascending aorta, adjacent to the right pulmonary artery (referred to as *distal defect*)

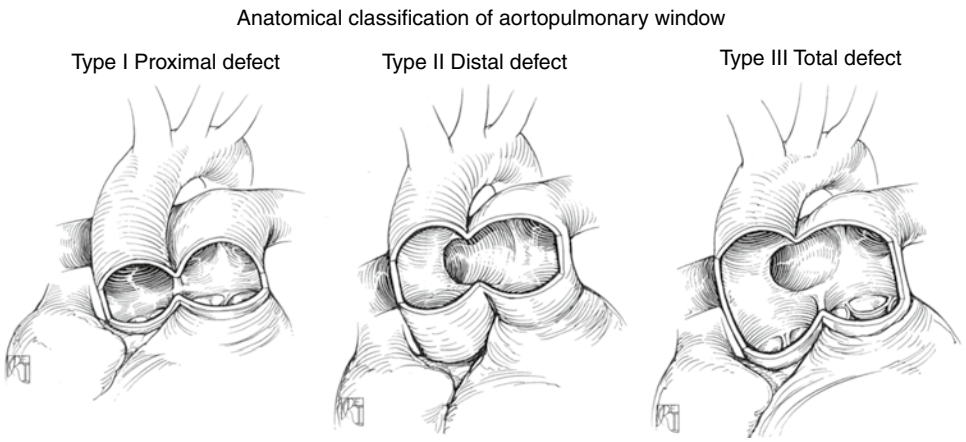

Fig. 13.11 Aortopulmonary window. Classification of aortopulmonary window as per Mori et al. (refer to text) (Reproduced with permission from Gaynor [133])

- Type III: a combination of Types 1 and II, involving the majority of the ascending aorta (referred to as *total defect*)

In a large review of cases, Kutsche and Van Mierop suggested that different developmental mechanisms likely account for the distinct forms of the defect [28]. Their analysis described three morphologic types as follows:

- A defect of small to moderate size with a more or less circular border located at the midpoint between the semilunar valves and pulmonary artery bifurcation
- A similarly located defect in which the border represents a helix
- A usually large defect without posterior (distal) border

Other classification schemes have been reported for anomalies of AP septation [29] and specifically consider the various types of AP windows [30].

Associated Defects

An AP window may occur in isolation, but more than half of the cases are associated with other cardiovascular malformations. Coexistent anomalies include PDA, septal defects at the atrial and/or ventricular levels, tetralogy of Fallot, double outlet right ventricle, type A interrupted aortic arch [31], right aortic arch, anomalous origin of the left coronary artery from the pulmonary artery [32], and coarctation of the aorta.

Pathophysiology

The magnitude of the shunt across an AP window relates to factors such as the size of the defect, pulmonary artery pressures, and relative resistances of the pulmonary and systemic circulations. Left-to-right shunting across the communication results in increased pulmonary blood flow, pulmonary hypertension, left-sided volume overload, and congestive symptoms. This condition is similar to the hemodynamic consequences of any other large abnormal vascular connection such as a PDA. An uncorrected communication can lead to the development of pulmonary vascular disease relatively early in life.

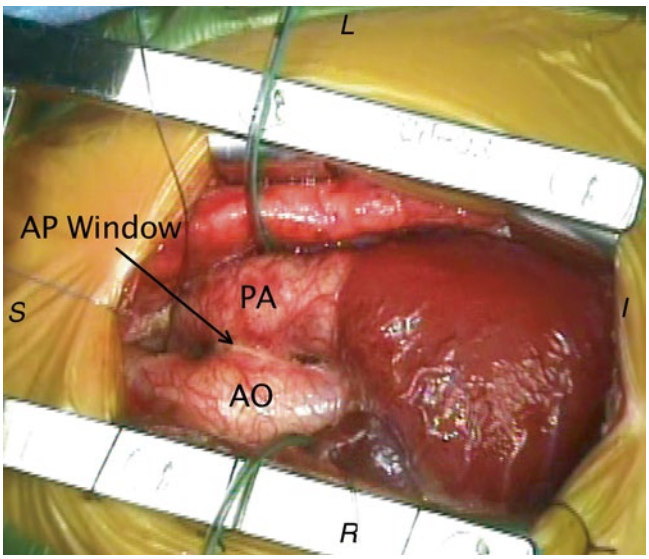

Fig. 13.12 Aortopulmonary window. Intraoperative photograph depicting the anatomical findings of an aortopulmonary (*AP*) window from a surgical perspective. *AO* aorta, *PA* pulmonary artery. *Image orientation*: *I* inferior, *L* left, *R* right, *S* superior

Management Considerations

Although successful transcatheter closure of an AP window has been reported [33–36], the standard treatment for this congenital lesion is considered to be surgical. The approach to this defect has evolved considerably over the years. In the past, simple ligation or division by suture closure was advocated [29, 37]; however, most centers now perform patch closure of the communication, using a median sternotomy and cardiopulmonary bypass (Fig. 13.12) [38, 39].

Applications of Transesophageal Echocardiography

As in many structural defects, the diagnosis of an AP window in the majority of cases is established by TTE alone [40–45]. Recently, the utility of 3D echocardiography has also been reported in the assessment of this anomaly [46].

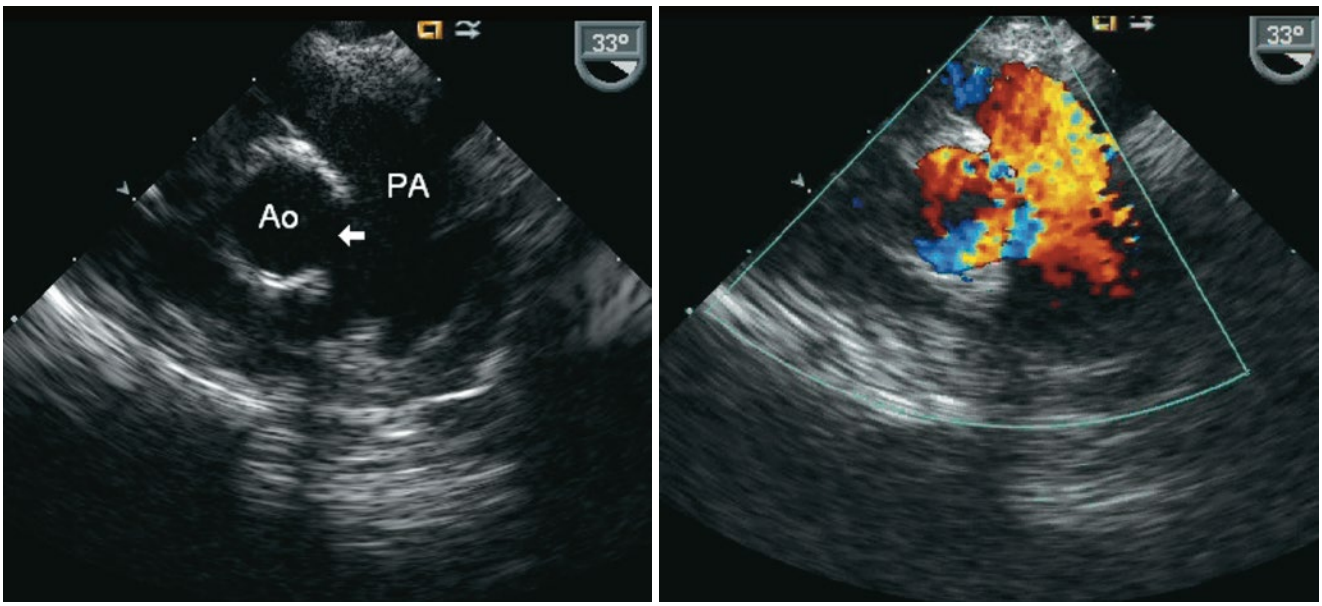

Fig. 13.13 Aortopulmonary window. Mid esophageal ascending aorta short axis view in infant with an aortopulmonary window. Note the echocardiographic drop out in the region between the arterial roots (*arrow*) corresponding to faulty aortopulmonary septation (*left panel*) and shunting across this region by color Doppler (*right panel*). *Ao* aorta, *PA* pulmonary artery

Rarely, additional imaging studies are required to further characterize the defect. TEE has been shown to be of benefit in the perioperative management of patients with AP communications such as an AP window [47].

Goals of TEE Prior to Surgical Intervention

Identification of an AP Window

The AP window is displayed by 2D imaging as a direct communication between the arterial trunks. It appears as a deficiency or absence (echocardiographic "dropout") of the wall normally interposed between the great arteries. The communication is usually large and frequently located along the anterior and leftward aspect of the aorta in the region where the great arteries are normally in apposition. The location and size of the defect, as well as its proximity to the semilunar valves are best evaluated in multiple views. Suggested TEE cross-sections to characterize an AP window are the UE PA LAX, UE Ao Arch SAX, and ME Asc Ao SAX views (Fig. 13.13 **left panel**, Video 13.6). The region of interest is the area of overlap between the great arteries or where they are seen in close proximity. The comprehensive evaluation of this defect may require the use of additional or non-standard TEE imaging planes, as may also be the case with other defects discussed throughout this textbook. For example, from the mid esophageal aortic valve long axis (ME AV LAX), mid esophageal long axis (ME LAX), mid esophageal ascending aortic long axis (ME Asc Ao LAX), and their respective modified views, the probe can be withdrawn slowly and sweeps performed by rotating the transducer in clockwise and counterclockwise fashions to display

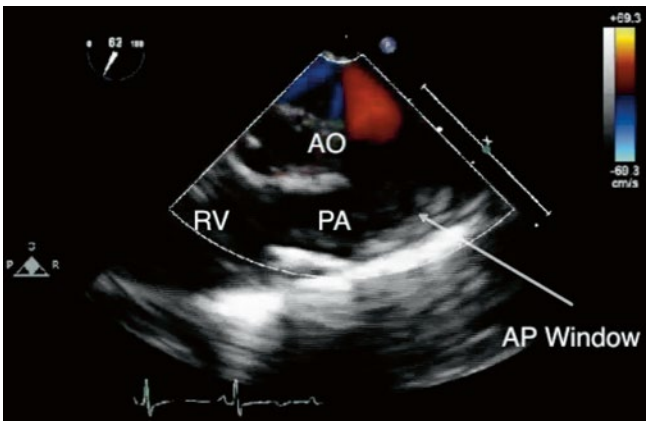

Fig. 13.14 Aortopulmonary window. View of the ascending aorta obtained at the upper esophageal level depicting an aortopulmonary (*AP*) window (*arrow*). *AO* aorta, *PA* pulmonary artery, *RV* right ventricle

the great arteries and the communication (Fig. 13.14, Video 13.7). The deep transgastric long axis (DTG LAX) and sagittal (DTG Sagittal) views, as well as modified respective views that display the great arteries as they cross each other, provide complementary information. It is important to note that an AP window would represent an extremely rare new finding on TEE; therefore, when a presumptive AP window has been identified for the first time on a TEE study, it is important to exclude potential diagnostic pitfalls that can mimic this defect, such as false echocardiographic dropouts in this region. Confirmatory information should be obtained, as discussed below.

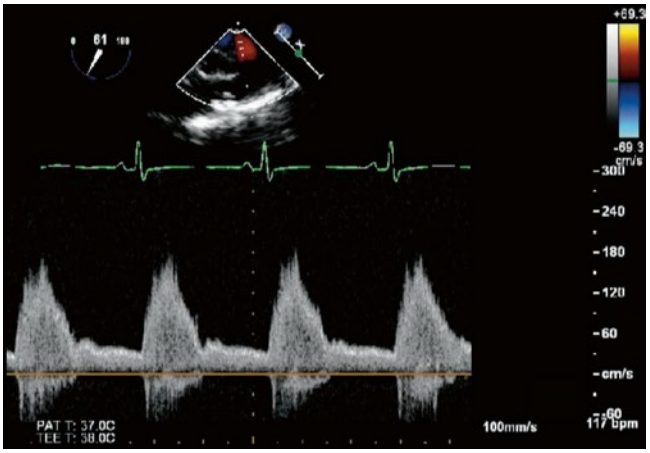

Fig. 13.15 Aortopulmonary window. Spectral Doppler tracing obtained in the same patient and same view as shown in Fig. 13.14. Note the systolic flow and continuous forward flow during diastole into the pulmonary artery

Characterization of Shunting Across AP Window

Color Doppler plays a very important role in the echocardiographic evaluation of an AP window. It verifies and characterizes the flow across the communication, providing qualitative information regarding shunt direction and magnitude. The same TEE views described in the identification of the defect can be used for this evaluation (Fig. 13.13 **right panel**, Videos 13.6 and 13.7). The spectral Doppler examination demonstrates antegrade continuous forward flow into the pulmonary artery near the area of the defect (Fig. 13.15). The presence of pulmonary hypertension at or near systemic levels is the norm for most large defects. In this case, low velocity, laminar, bidirectional (predominantly left-to-right) shunting across the communication reflects the negligible systolic pressure gradient between the systemic and pulmonary beds. This condition may render the identification of shunting somewhat difficult. Adjustment of the Nyquist limit for the color Doppler scale enhances the detection of low velocity flows and can be used to facilitate the detection of shunting across the communication. It is important to distinguish the low velocity color flow signal across an AP window from the "bleeding" of color flow sometimes seen across the walls of the aorta and pulmonary artery in a normal heart. Interrogation of the ascending aorta near the communication or of the descending thoracic aorta may display diastolic flow reversal in the presence of low pulmonary vascular resistance. It is similar to the nature of descending aortic flow in a moderate to large-sized PDA, and serves as indirect evidence of the presence of an AP communication, although it is not specific of the type. Smaller, restrictive defects can display a turbulent color flow Doppler pattern that corresponds to high velocity, continuous left-to-right shunting across the area.

Estimation of Pulmonary Artery Systolic Pressure

As indicated, flow across large communications displays low velocity consistent with elevated pulmonary artery pressures. Smaller defects result in pressure restriction, displaying flow aliasing (mosaic pattern) by color Doppler and high velocity flow by spectral Doppler. The peak velocity of the continuous wave Doppler signal can be used to estimate PASP (as described for a PDA). The peak velocity of the tricuspid regurgitant jet, if present, can also be applied to estimate RVSP, as noted previously. Additional findings that may provide insight into the extent of pulmonary artery pressure elevation include: motion and configuration of the interventricular septum, right ventricular wall thickness, and degree of right ventricular dilation.

Additional Applications

Depending on the presence of associated defects, additional aspects of the anatomy should be examined using corresponding TEE views as necessary. The hemodynamic effects of the volume load result in dilation of the pulmonary arteries and left-sided cardiac structures. The nature of the runoff associated with an AP window may result in low systemic diastolic pressures, low coronary perfusion pressures, and the potential for coronary ischemia and/or myocardial dysfunction. Thus, it is essential to assess both global and segmental left ventricular systolic function in the preoperative evaluation. This assessment is best performed in the transgastric mid short axis (TG Mid SAX), transgastric basal short axis (TG Basal SAX), transgastric two chamber (TG 2 Ch), mid esophageal four chamber (ME 4 Ch), mid esophageal two chamber (ME 2 Ch), and ME LAX views (also refer to Chap. 5).

Intraoperative Monitoring

In rare cases, depending upon the location of the AP window and other factors such as the size and length of the communication, consideration may be given to using a surgical approach that obliterates the communication without the need for cardiopulmonary bypass. In this setting, TEE is valuable for intraoperative monitoring and assessing the results of surgery. In addition, TEE is extremely useful for evaluating global and segmental ventricular function as well as left ventricular preload, and also for excluding the presence of intracardiac/intravascular air.

Goals of TEE After Surgical Intervention

Assessment of the Repair

Obliteration of the abnormal AP connection in most cases requires patch closure (Fig. 13.16, Video 13.8). The post-repair TEE assessment should explore potential residual shunting and patency of the arterial roots to exclude

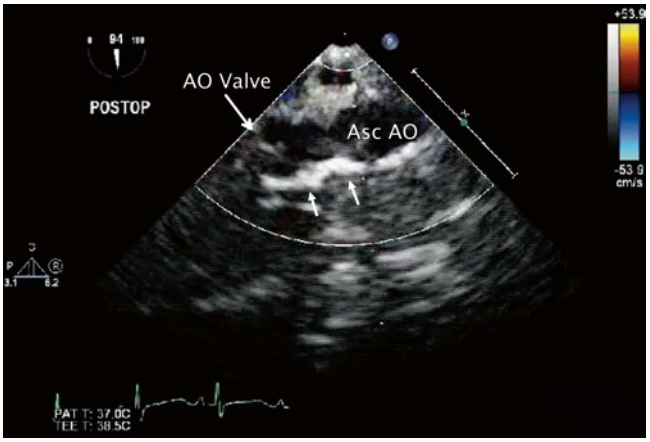

Fig. 13.16 Aortopulmonary window. Postoperative transesophageal echocardiogram in the mid esophageal ascending aortic long axis view depicts the bright region along the wall of the ascending aorta (*Asc AO*) by two-dimensional imaging corresponding to the pericardial patch (*arrows*) utilized to close the aortopulmonary defect in the patient depicted in Figs. 13.14 and 13.15. *AO* aortic

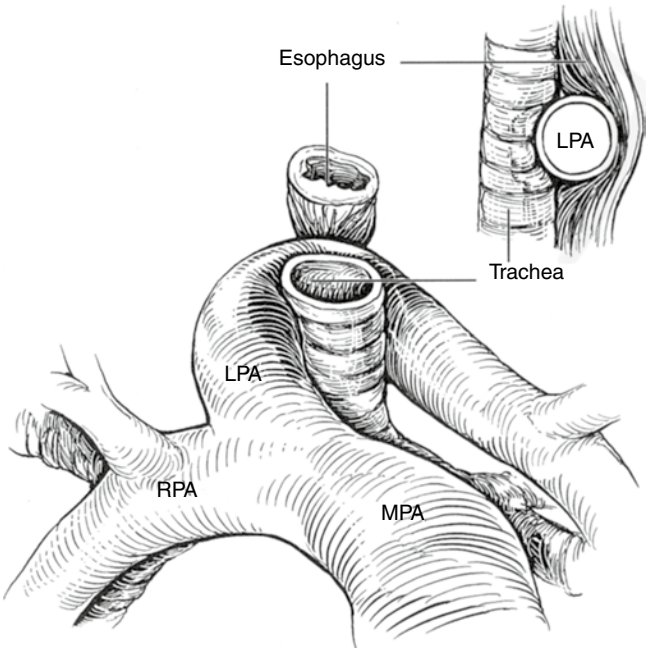

Fig. 13.17 Pulmonary artery sling. Graphic depiction of a pulmonary artery sling. *LPA* left pulmonary artery, *MPA* main pulmonary artery, *RPA* right pulmonary artery. *Inset*, lateral view of anterior compression of esophagus (Reproduced with permission from Backer et al. [134])

obstruction of either the aorta or pulmonary artery. This represents the primary reason for morbidity in this lesion [48]. Semilunar valve competence also should be examined, as regurgitation can result from the repair, particularly if the AP window is proximally located near the semilunar valves.

Additional Applications

The adequacy of the surgical intervention with regard to coexistent lesions should also be examined thoroughly, as well as other relevant aspects of any postbypass evaluation (e.g., ventricular systolic function, atrioventricular and semilunar valve regurgitation).

Anomalies of the Branch Pulmonary Arteries

Anomalous Origin of the Left Pulmonary Artery from the Right Pulmonary Artery

Anatomic Features

In this vascular anomaly, also referred to as a *pulmonary artery sling* [49], the left pulmonary artery originates abnormally from the proximal right pulmonary artery [50]. The course of the left pulmonary artery is such that it arises from the posterior aspect of the right pulmonary artery, crosses above the right mainstem bronchus, and travels posteriorly between the trachea and esophagus towards the left hilum (Fig. 13.17). Hypoplasia of the left pulmonary artery often is seen, whereas some degree of dilation of the right pulmonary artery is the norm. The boundaries of the trachea in this setting consist of the main pulmonary artery anteriorly, the left pulmonary artery to the right and posteriorly, and the ductus or ligamentum arteriosum to the left. In contrast to other vascular anomalies such as a double aortic arch or right aortic arch with a left ductus/ligamentum, a pulmonary artery sling, does not represent a true complete anatomic ring. However, this lesion is frequently considered within the context of vascular anomalies causing a ring. The pathology is attributed to a developmental malformation, although several instances have been reported in patients with a relatively recently described genetic syndrome (Mowat-Wilson) [51, 52].

Associated Defects

A significant number of patients with this malformation (more than 50 %) have complete tracheal rings and/or other tracheobronchial abnormalities (Fig. 13.18) [53, 54]. This condition is associated with tracheal narrowing, and, if significant, the stenosis can result in airway obstruction [53, 55–57]. Tracheomalacia is present in nearly all patients. Additional cardiovascular pathology also is a frequent finding. The most commonly associated defects include intracardiac communications at either the atrial or ventricular levels, PDA, and tetralogy of Fallot [57–59]. Other extracardiac abnormalities, such as hypoplasia and agenesis of the right lung, have also been reported [53].

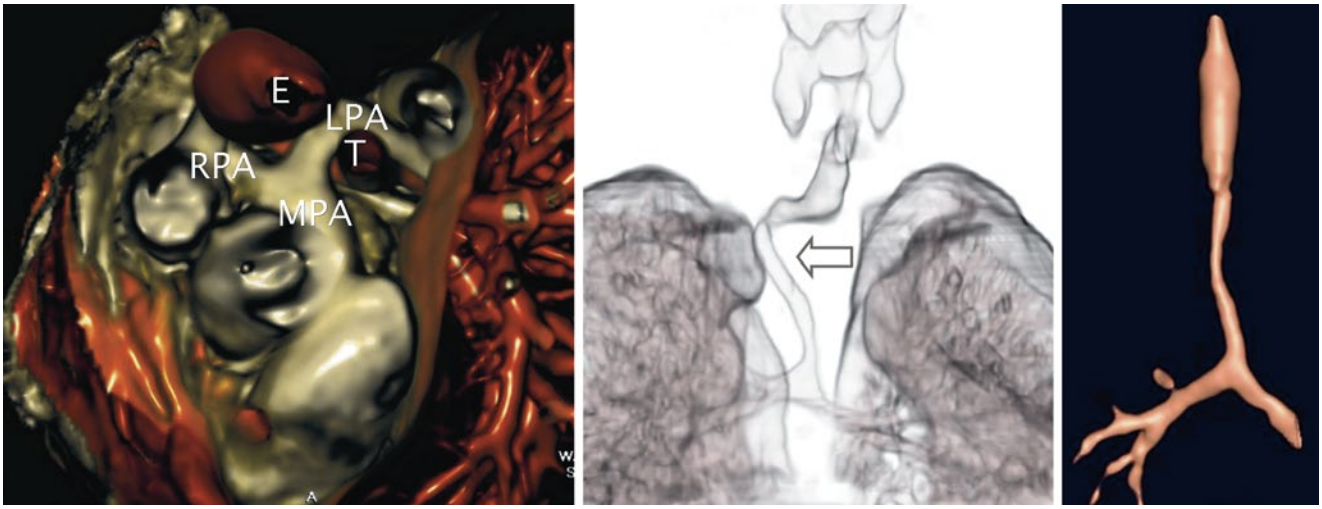

Fig. 13.18 Pulmonary artery sling. Three-dimensional rendered images obtained by computed tomography in a patient with anomalous origin of the left pulmonary artery from the right pulmonary artery. *Left panel*, anomalous left pulmonary artery (*LPA*) as it arises from the posterior aspect of the right pulmonary artery (*RPA*) and courses behind the trachea (*T*) and anterior to the esophagus (*E*) to reach the left hilum. Examples of associated tracheobronchial anomalies that can be seen in this vascular anomaly include a "corkscrew-type" (*arrow*) deformity (*middle panel*) and complete tracheal rings with absence of the membranous trachea causing airway narrowing (*right panel*). Both of these entities frequently result in airway compromise. *MPA* main pulmonary artery (Images by courtesy of Rajesh Krishnamurthy, MD)

Pathophysiology

Although a pulmonary artery sling may present as an incidental finding, the unusual course of the anomalous vessel behind the trachea or right bronchus frequently leads to distortion of the tracheobronchial tree, airway compression, and respiratory symptoms in early infancy. The airway compromise occurs regardless of the presence of associated congenital tracheal stenosis. In some cases, the anomalous left pulmonary artery displays stenosis and/or hypoplasia. The clinical manifestation of this defect can be influenced significantly by the presence of coexistent anomalies.

Management Considerations

The high incidence of tracheal anomalies in this lesion requires comprehensive airway assessment to formulate suitable management plans [53, 60]. The surgical approach in most cases consists of left pulmonary artery division and reimplantation into the main pulmonary artery, allowing for the vessel to be positioned anterior to the trachea. This procedure is now accomplished at most centers via a median sternotomy approach using cardiopulmonary bypass [53, 61]. Concomitant repair of tracheal stenosis and associated intracardiac anomalies is performed as indicated [62–65]. If short-segment tracheal stenosis is present, resection of the involved region is performed; while the trachea is divided, the left pulmonary artery can be translocated anterior to the trachea, obviating the need for surgical division and left pulmonary artery reimplantation.

Applications of Transesophageal Echocardiography

In addition to TTE, other imaging modalities such as chest CT scanning and MRI play important roles in identifying and defining the details of the anatomy in the patient with a pulmonary artery sling prior to surgical intervention [54, 60, 66–74]. At the same time, these additional imaging studies allow for the airway to be examined. The characteristic finding is that of the abnormal origin and course of the vessel. Depending on the particular diagnostic study, an anterior indentation of the esophagus is seen, in contrast to other types of vascular rings, which produce a posterior indentation of the esophagus.

Because of concerns related to frequently associated airway pathology and potential for respiratory decompensation due to esophageal instrumentation, serious consideration of the risk-benefit ratio should be given prior to the use of TEE in affected patients, particularly considering that the anatomic abnormalities usually have been thoroughly outlined. Epicardial imaging should be considered a potentially safer alternative in this case. Another reason for hesitation relates to possible alterations in pulmonary blood flow caused by vascular compression of the anomalous vessel, which can be impinged between the trachea and the esophageal probe. All these factors have discouraged the routine use of TEE in this anomaly and likely account for the limited experience. The discussion that follows highlights known or potential applications of TEE when used in this setting.

Goals of TEE Prior to Surgical Intervention

Characterization of the Anomaly

TEE can confirm or refine the preoperative diagnosis in patients undergoing surgical repair of a pulmonary sling, particularly if concomitant defects are present. The ME Asc Ao SAX and UE PA LAX views using sweeps of the imaging plane obtained by clockwise-counterclockwise rotation

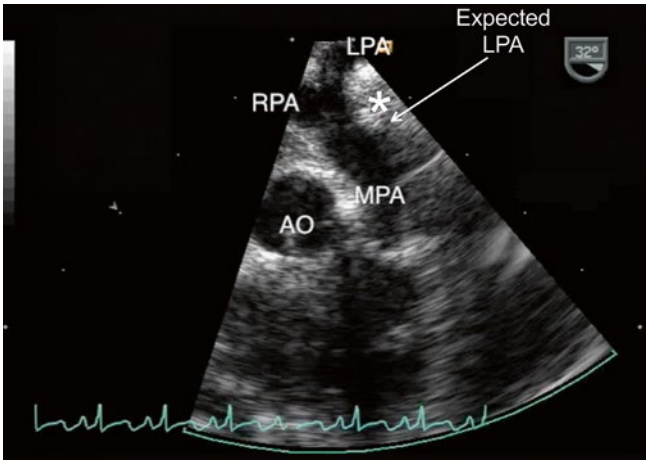

Fig. 13.19 Pulmonary artery sling. Upper esophageal pulmonary artery long axis view of a pulmonary artery sling. The image demonstrates the abnormal takeoff of the left pulmonary artery (*LPA*) from the right pulmonary artery (*RPA*). Note the lack of a normal main pulmonary artery bifurcation that typically would occur more proximally relative to the pulmonary valve (approximate expected site of normal LPA origin noted). The anomalous course of the LPA with respect to the trachea (*white asterisk*) is shown. *AO* aorta, *MPA* main pulmonary artery

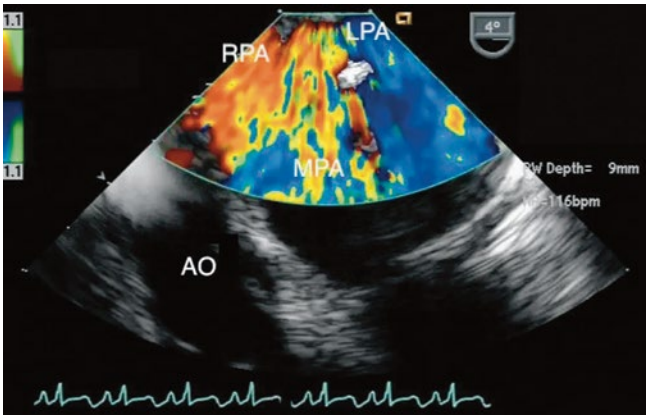

Fig. 13.20 Pulmonary artery sling. Color Doppler image of the same cross-section depicted in Fig. 13.19 obtained in a zoom mode. Note flow into the left pulmonary artery (*LPA*) as it arises from the right pulmonary artery (*RPA*). *AO* aorta, *MPA* main pulmonary artery

to visualize the main and branch pulmonary arteries should display the vascular anomaly. In this interrogation, only the right pulmonary artery origin from the main pulmonary artery is visualized if one scans proximally, in contrast to the normal pulmonary artery bifurcation. If the right pulmonary artery is examined slightly more distally, the origin of the left pulmonary artery might be seen posteriorly (Fig. 13.19, Video 13.9). Although the pulmonary artery bifurcation may appear to have moved rightwards, this finding should not be interpreted as normal. The 2D examination should allow for measurements to be made of the pulmonary arteries to assess for the degree of vessel dilation, stenosis, or possible associated hypoplasia. Doppler interrogation using spectral and color flow modalities facilitates characterization of the anomaly (Fig. 13.20, Video 13.10). In addition to the cross-sections described above, deep transgastric imaging (DTG LAX and DTG Sagittal views) may on occasion assist in the evaluation of a vascular sling, particularly if scanning sweeps are performed.

The findings in a pulmonary artery sling should not to be confused with those of an early takeoff of the right upper lobe pulmonary artery or other vascular anomalies in which the left pulmonary artery originates from the systemic circulation (to be discussed in the section that follows). The demonstration of the origin and course of the left pulmonary artery is essential in this distinction. On TTE, a PDA or left atrial appendage can be mistaken for a normal pulmonary artery, leading to a diagnostic error [67], and it may also confound the TEE evaluation. Partial forms of pulmonary artery sling have been described in which the left pulmonary artery arises from the bifurcation normally, but one of the left lobar branches originates from the right pulmonary artery and courses in anomalous fashion similar to that of the classic form of pulmonary artery sling [75, 76]. This lesion has been identified by transthoracic imaging and, although not yet documented, TEE may also be able to assist in the characterization of this malformation. The finding of a 'normal bifurcation' in this defect may also confound the examination of a partial sling if the echocardiographer is not familiar with this anomaly and the more distal right pulmonary artery is not examined to identify the anomalous origin of the lobar branch.

TEE has been shown to be of benefit in the identification of the abnormal origin and unusual path of the left pulmonary artery in this lesion, but some limitations have been identified [77]. Although color Doppler echocardiography enhances the assessment, the origin of an anomalous vessel or entire course behind the trachea may not be readily delineated, even using the combination of standard and modified scanning planes. Spectral Doppler can be used to provide information regarding severity of pulmonary artery obstruction if present. The caveat to this approach is that optimal beam alignment may not be feasible, and the severity of the obstruction can be underestimated if flow to the distal pulmonary vascular bed is limited.

Additional Applications

TEE in this setting is of value in the evaluation of associated defects (such as tetralogy of Fallot) and for intraoperative monitoring [78].

Goals of TEE After Surgical Intervention

Postsurgical Assessment

If TEE is used, the postoperative study should assess the repair by examining the anastomotic connection of the left

pulmonary artery to the main pulmonary artery and the nature of blood flow across the corresponding site. This assessment is important considering that tension can be created at this site or a left pulmonary arterioplasty may be required to address associated branch hypoplasia. The results of additional surgical interventions for coexistent defects should also be examined.

Anomalous Origin of a Branch Pulmonary Artery from the Aorta

Anatomic Features

Anomalous origin of a branch pulmonary artery branch from the aorta is a rare congenital malformation. In this anomaly, a main pulmonary segment arises normally from the right ventricle, but only one branch emerges from the pulmonary artery confluence, and the controlateral branch originates from the ascending aorta, resulting in discontinuity between the pulmonary arteries.

Several theories have been proposed to explain the developmental alterations leading to this anomaly, but no consensus has been reached [79–81]. Although this malformation has also been referred to as *hemitruncus*, anatomically it should be distinguished from truncus arteriosus because, in contrast to a single semilunar valve, two semilunar valves are present in this setting. This anomaly represents less than 0.1 % of all CHD.

Although the anomaly described above of an aortic origin of a branch pulmonary artery represents the most common form of this lesion [82], the anomalous vessel can originate elsewhere [83]. In some cases, the pulmonary artery originates from unusual locations, particularly in the context of complex cardiovascular malformations [84]. It has been proposed that proximal anomalous origin of a pulmonary artery from the ascending aorta and anomalous origin from the innominate artery, also referred to as *absent* or *occult pulmonary artery* [85, 86], are two distinct and separate entities from the standpoint of embryology, clinical presentation, and treatment [87–89].

In a review of the pathologic anatomic features and associated cardiovascular anomalies of patients with anomalous origin of one pulmonary artery, the following observations were made: (1) in most cases, the anomalous origin was that of the right pulmonary artery and (2) the anomalous right pulmonary artery typically arose from the posterior aspect of the ascending aorta in immediate proximity to the aortic valve, or, less commonly, the vessel originated from the lateral aspect of the ascending aorta just proximal to the innominate artery [79]. The anomalous vessel may arise from the left, anterior, or posterior wall of the ascending aorta, innominate/subclavian artery, ductus arteriosus, aortopulmonary collateral vessel, or descending aorta [90].

The discussion that follows focuses primarily on anomalous origin of the pulmonary artery from the ascending aorta, the malformation that most likely benefits from TEE, and briefly addresses related lesions or variants as described above.

Associated Defects

When the right pulmonary artery arises from the ascending aorta, in most instances there is a left aortic arch. In contrast, in the case of an anomalous left pulmonary artery, frequently the arch is right-sided [79]. Associated defects include simple lesions such as a PDA and more complex defects include conotruncal anomalies [91]. Tetralogy of Fallot and aortic arch anomalies have been frequently found in anomalous origin of the left pulmonary artery [79, 90, 92]. Normal cardiac anatomy has been reported in some cases.

Pathophysiology

The clinical features of anomalous origin of a branch pulmonary artery from the ascending aorta usually are those characteristic of pulmonary overcirculation and congestive heart failure [93]. In most infants, evidence of pulmonary hypertension is seen [94]. It is of interest that pulmonary artery pressures are at systemic or suprasystemic levels not only in the bed perfused by the anomalous vessel but also in the controlateral lung supplied by the pulmonary artery that arises from the right ventricle. The rapid development of pulmonary vascular disease, although recognized as a major cause of morbidity in the past [95], rarely occurs in the current era because symptoms prompt medical attention in most affected infants.

If the anomalous pulmonary artery arises near the innominate/subclavian artery, a high incidence of stenosis at the origin of vessel has been observed [82]. If the anomalous vessel has a ductal origin, eventual isolation occurs at the time of ductal closure. The clinical presentation in the latter case varies and may represent an incidental finding in some patients; for example, it may be diagnosed after evaluation of an abnormal chest radiograph in children or it may be identified later in life.

Management Considerations

The management of this malformation depends on the nature of the pathology. If the anomalous vessel arises proximally in the ascending aorta and there is no restriction to blood flow, as is usually the case, early surgical intervention is indicated [91, 94, 96–98]. Primary repair involves reimplantation of the anomalous pulmonary artery into the pulmonary trunk (Fig. 13.21) [90, 99].

If there is evidence of restriction to blood flow and/or associated hypoplasia, or isolation of the vessel, various strategies have been used in order to attempt to ‘resuscitate’ the anomalous vessel. The main goal is to restore normal antegrade flow to the pulmonary artery [100, 101]. The

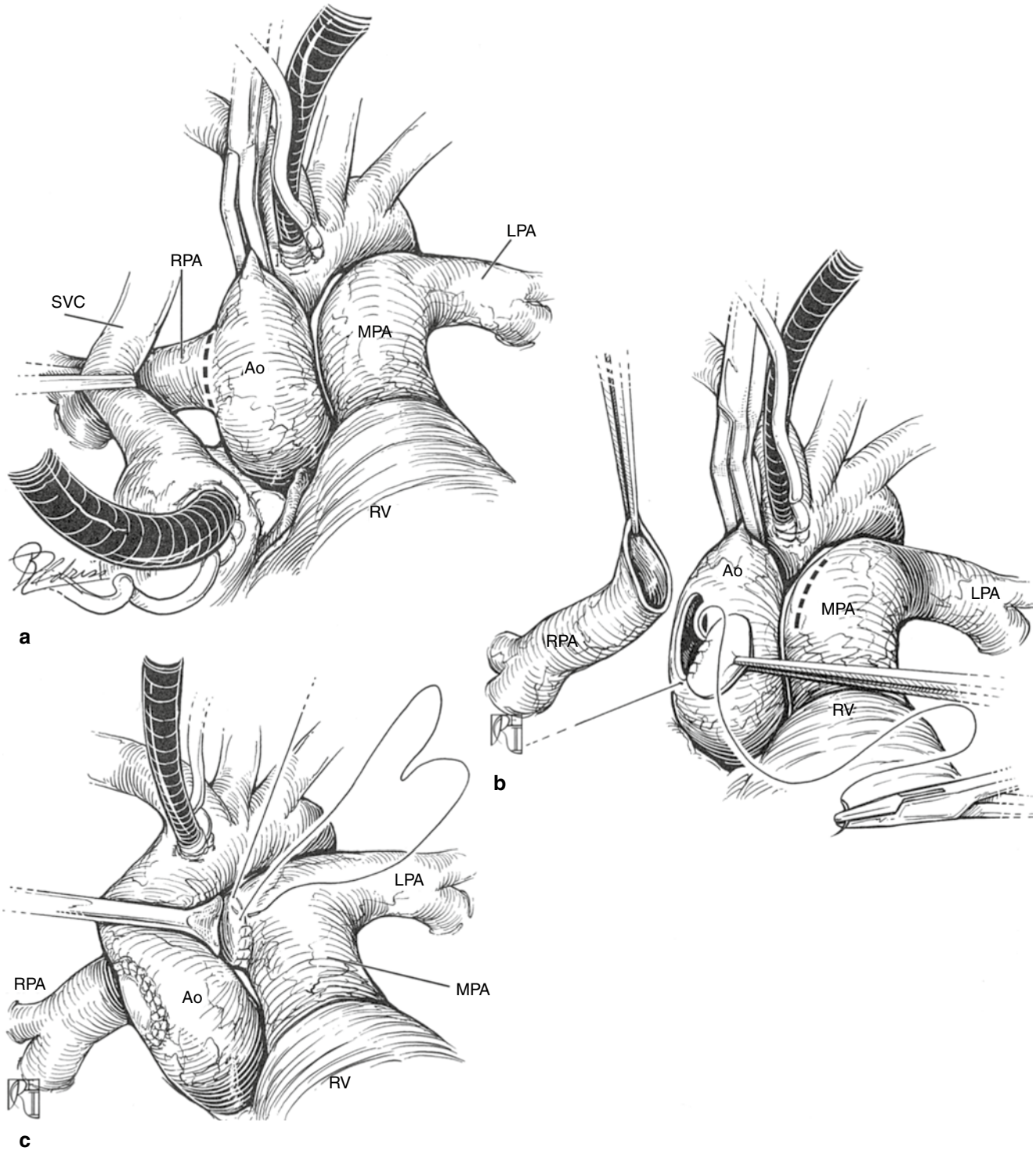

Fig. 13.21 Aortic origin of pulmonary artery. Graphic depiction of surgical repair for aortic origin of right pulmonary artery (RPA). Panel **a** displays the anomaly after cannulation for cardiopulmonary bypass. Panel **b** shows detachment of the RPA from the aorta (Ao) and patch closure of the ensuing wall defect. Panel **c** illustrates the direct anastomosis of the RPA into the main pulmonary artery (MPA) to establish continuity with the left pulmonary artery (LPA). *RV* right ventricle, *SVC* superior vena cava (Reproduced with permission from Gaynor [133])

approach might involve resection of a stenotic segment and/or placement of an interposing aortopulmonary graft to promote growth, followed by eventual takedown of the anomalous vessel and reestablishment of continuity between the pulmonary arteries. In some cases of focal stenosis at the vessel origin, a single-staged approach can be used by resecting the stenotic segment and incorporating the anomalous vessel into the main pulmonary artery.

Applications of Transesophageal Echocardiography

In the classic form of this lesion, the diagnosis usually is established by transthoracic imaging [41, 95, 102]. If the anomalous pulmonary artery cannot be identified by echocardiography, as may be the case in older children with isolation of the aberrant vessel or in adult patients, additional imaging studies are undertaken to confirm the diagnosis and to attempt to delineate the vessel. In some cases, this approach may include cardiac catheterization and angiography [100].

Goals of TEE Prior to Surgical Intervention

Characterization of the Anomaly

In this malformation, 2D TEE demonstrates two distinct outflow tracts and semilunar valves. This condition can be assessed in a combination of planes allowed by the UE PA LAX, mid esophageal aortic valve short axis (ME AV SAX), ME AV LAX, ME LAX, and ME RV In-Out views. In the normal heart, the pulmonary artery bifurcation typically is seen in the ME Asc Ao SAX, UE PA LAX, and transgastric views (Figs. 13.22 and 13.23; Videos 13.11 and 13.12). In the setting of anomalous origin of a pulmonary artery from the ascending aorta, the bifurcation is absent and only a single branch arises from the pulmonary trunk (Fig. 13.24, Video 13.13).

When the anomalous branch originates near the aortic valve or from a relatively proximal site in the aortic root, its origin and immediate proximal course can be demonstrated in the ME AV LAX, ME Asc Ao LAX, ME Asc Ao SAX, or equivalent views if a biplane probe is used (Fig. 13.25, Videos 13.14 and 13.15). In some cases, as the probe is withdrawn from the ME LAX to the ME Asc Ao LAX, a relatively distal origin of an anomalous vessel can be seen (Fig. 13.26, Video 13.16). If the anomalous pulmonary branch originates from the innominate or subclavian arteries or elsewhere, TEE is not adequate to define or characterize the pathology in detail.

The exam is facilitated by color Doppler flow mapping, displaying discontinuity between the pulmonary artery branches and flow from the aorta into the anomalous branch (Fig. 13.26, Video 13.16). Sampling of the aorta distal to the communication demonstrates retrograde flow in diastole, consistent with the runoff physiology.

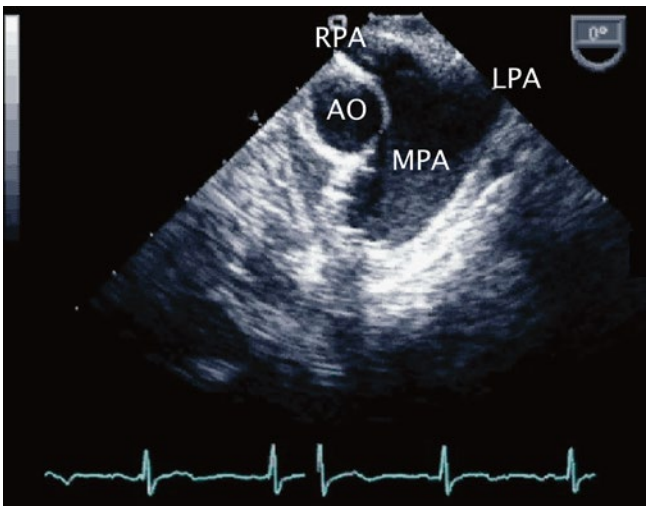

Fig. 13.22 Main pulmonary artery bifurcation. Normal branching of the main pulmonary artery (*MPA*) into the right (*RPA*) and left (*LPA*) pulmonary arteries as imaged from the upper esophageal pulmonary artery long axis view. *AO* aorta

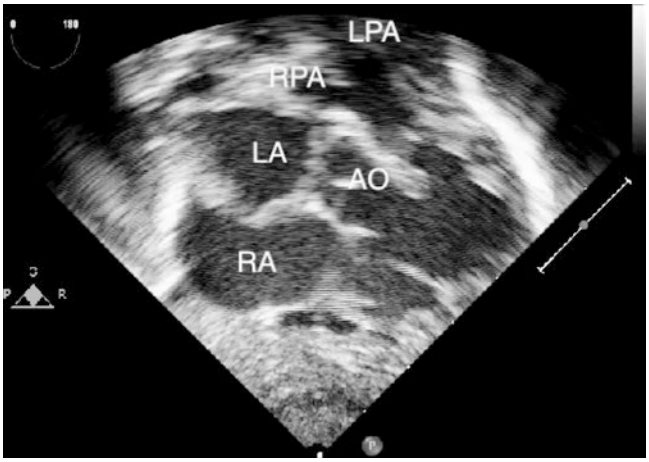

Fig. 13.23 Main pulmonary artery bifurcation. Modified deep transgastric image obtained in an infant with double outlet right ventricle and a subaortic ventricular septal defect to demonstrate the normal main pulmonary artery bifurcation as seen in cross-section from this window. *AO* aorta, *LA* left atrium, *LPA* left pulmonary artery, *RA* right atrium, *RPA* right pulmonary artery

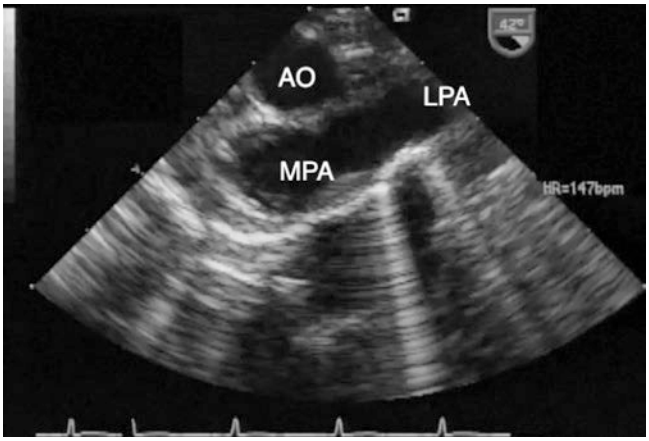

Fig. 13.24 Absent main pulmonary artery bifurcation in aortic origin of right pulmonary artery. Upper esophageal pulmonary artery long axis view displaying the left pulmonary artery (*LPA*) as it arises from the main pulmonary artery (*MPA*). Note the absence of the normal pulmonary artery bifurcation in this patient with anomalous origin of the right pulmonary artery from the aorta (*AO*)

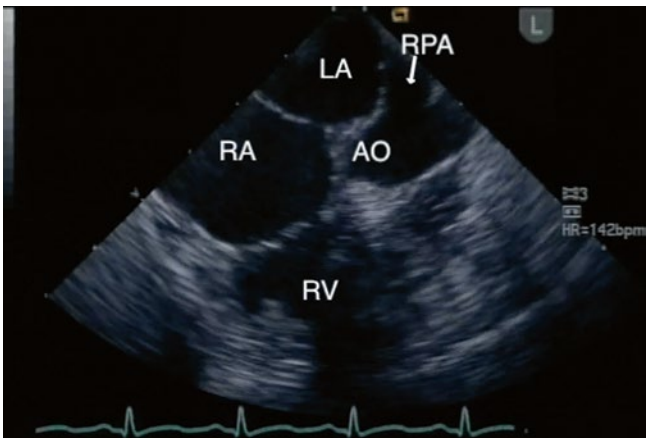

Fig. 13.25 Aortic origin of right pulmonary artery. Image obtained in a long axis plane using a biplane transesophageal probe displaying anomalous origin (*arrow*) of the right pulmonary artery (*RPA*) from the aorta (*AO*). *LA* left atrium, *RA* right atrium, *RV* right ventricle

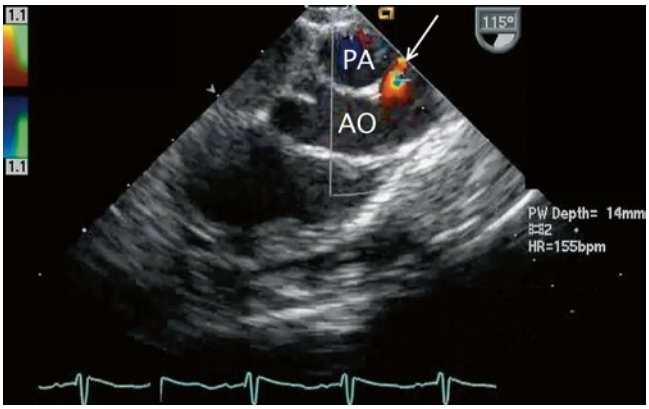

Fig. 13.26 Aortic origin of right pulmonary artery. Mid esophageal ascending aortic long axis view with color Doppler displaying anomalous origin of right pulmonary artery from the ascending aorta (*AO*). Note the more distal origin of the anomalous vessel (*arrow*) as compared to that seen in the patient shown in Fig. 13.25. *PA* main pulmonary artery

The echocardiographic features of anomalous origin of a pulmonary artery from the ascending aorta should be distinguished from those of other lesions. In the case of an AP window, a normal main pulmonary artery bifurcation is present and continuity between the pulmonary arteries is seen. This observation is in contrast to the lack of a pulmonary artery confluence seen when a branch pulmonary artery arises elsewhere. When a pulmonary artery arising anomalously from the aorta is the lone defect, there will still be two arterial roots and two semilunar valves present. This contrasts to truncus arteriosus, in which a single semilunar valve, corresponding to a single arterial root, gives rise to the systemic, pulmonary, and coronary circulations. It is important to remember that discontinuous pulmonary arteries can also exist in the setting of truncus arteriosus, specifically Type A3 of the Van Praagh classification (Chap. 12) in which the right pulmonary artery arises from the truncus arteriosus, but the left pulmonary artery arises from a ductus arteriosus. This underlines the importance of determining whether one or two semilunar valves are present.

Additional Applications

As mentioned, pulmonary hypertension (in both lungs) is a common finding in patients with proximal aortic origin of a branch pulmonary artery. As this is the most frequent variant of this class of defects, the TEE examination should utilize 2D and spectral Doppler to attempt to estimate the pulmonary artery pressures (Fig. 13.9, Video 13.4). This determination can be accomplished by assessing the flow velocities corresponding to the tricuspid or pulmonary regurgitant jets, the gradient across the junction of the aorta and anomalous vessel, the configuration of the interventricular septum, and the thickness of the right ventricular wall. Additional benefits of TEE include intraoperative monitoring and evaluation of associated defects.

Goals of TEE After Surgical Intervention

Postsurgical Assessment

After the anomalous branch pulmonary artery has been reimplanted, the TEE evaluation should focus on 2D imaging and Doppler analysis of the main pulmonary artery, region of newly created confluence, and both branches, particularly the reconstructed anomalous vessel. The same TEE views used for the presurgical examination can be applied. It is important to document patency of the vessel and characterize the nature of the flow both at the site of anastomosis and further distally. If there was significant preoperative pulmonary hypertension, an attempt should be made to reassess the pulmonary artery pressures following surgery, using the methods outlined above. The adequacy of interventions performed for concomitant pathology should also be assessed. All of the standard postoperative monitoring evaluations previously mentioned—such as cardiac function, intracardiac air, ventricular filling—should be carefully performed.

The postoperative assessment can be particularly challenging in the case of a hypoplasic anomalous pulmonary artery. This may be due to factors such as the relatively small size of the vessel, even after arterioplasty, and/or distortion of mediastinal structures due to underdevelopment of the lung parenchyma, that may not allow for optimal 2D imaging. Color Doppler can enhance this examination, although the frequently associated collateral circulation to the corresponding distal pulmonary vasculature can confuse the characterization of flow related to the reconstructed vessel.

Anomalies of the Aortic Arch

When used in patients with aortic arch anomalies, the primary goal of TEE is the evaluation of coexistent defect(s), rather than to focus on the aortic arch pathology itself, because of

the limitations of the imaging modality. The difficulty stems from the anterior position of the air-filled trachea relative to the esophagus making the comprehensive examination of the distal ascending aorta and proximal aortic arch challenging, if not impossible. Despite these shortcomings, the discussion that follows highlights the role of TEE in patients with coarctation of the aorta and interrupted aortic arch. Other aortic arch abnormalities/variants are not discussed in this chapter because the applications of TEE for their specific assessment are limited, have not been described, or the use of this imaging approach is considered contraindicated. These anomalies include vascular rings (e.g. double aortic arch), cervical aortic arch, and anomalous origin of a subclavian artery. For these lesions, modalities such as TTE, MRI, chest CT, and angiography are considered diagnostic. In the case of aortic arch laterality variants such as a right aortic arch, although TEE can define/confirm aortic arch sidedness this does not represent a major application of the technology. The branching pattern cannot be well defined due to the fact that the arch vessels are difficult to image adequately and consistently.

Coarctation of the Aorta

Anatomic Features

In coarctation of the aorta (CoA), there is narrowing of the aortic lumen, most frequently in the region of insertion of the ductus arteriosus/ligamentum arteriosum. This defect accounts for 5–8 % of all congenital cardiovascular pathologies and has a higher prevalence in males. The constriction in CoA may take the form of a discrete infolding-like posterior shelf or a diffuse hourglass narrowing of the distal arch. An elongated, narrowed aortic outflow tract is often associated with hypoplasia of the transverse arch and aortic isthmus, in which case other structural cardiac malformations can be present. Thus, CoA is considered to represent a disease spectrum. This malformation occurs in sporadic fashion; however, genetic factors are implicated because CoA is present in more than a third of females with Turner syndrome.

Traditionally, CoA was classified into two types, the preductal (infantile) or postductal (adult) forms (Fig. 13.27). The infantile type of CoA referred to the lesion in the neonate characterized by a long, tubular hypoplastic segment of the aortic arch and large ductus supplying the distal descending aorta. The adult form, presenting after infancy, was described as a shelf-like infolding of the posterior aortic wall into the lumen either at or distal to the ligamentum. This discrete obstructive shelf represents the most common form of this lesion, affecting the region where the isthmus, ductus arteriosus, and descending aorta join together; it is currently referred to as *juxtaductal* CoA.

Associated Defects

CoA may be seen in isolation (with or without PDA), in which case it is referred to as *simple* CoA, or coexisting with other defects, also known as *complex* CoA. Associated malformations include ventricular septal defect(s), bicuspid aortic valve, aortic stenosis, atrioventricular septal defect, double

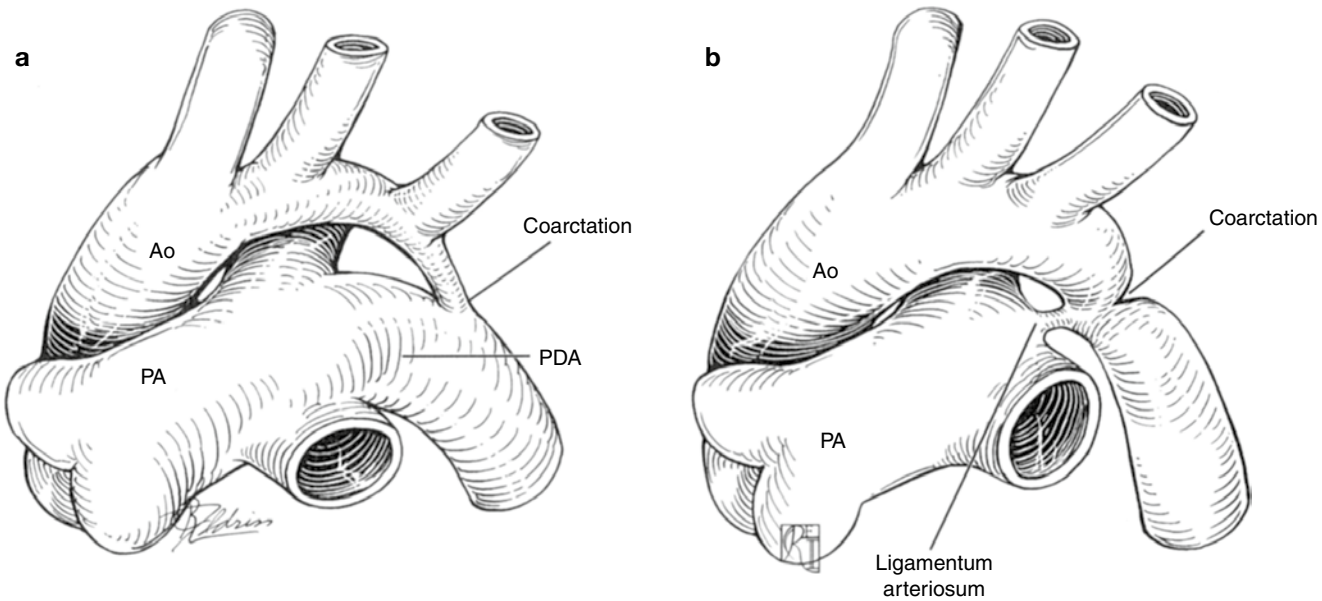

Fig. 13.27 Coarctation of the aorta. Graphic illustration of coarctation of the aorta. (**a**) Infantile, or "preductal", coarctation of the aorta. The patent ductus arteriosus (*PDA*) provides the majority of blood flow to the descending aorta. There is tubular narrowing of the transverse arch and a small aortic isthmus. (**b**) Adult, or "postductal", coarctation of the aorta. The area of narrowing is actually juxtaductal and consists of a prominent posterior ridge projecting into the lumen. The ductus arteriosus has closed and is now a ligamentum arteriosum. *Ao* aorta, *PA* pulmonary artery (Reproduced with permission from Backer et al. [135])

outlet right ventricle, transposition of the great arteries, mitral valve abnormalities, and various other types of left-sided obstructive lesions. Some investigators have proposed that the etiology and pathophysiology of bicuspid aortic valve and CoA are closely related and represent a spectrum of a more generalized arteriopathy rather than discrete pathologies [103]. Dilated aortic root and intracranial aneurysms are known to be associated with coarctation [104]. CoA may also be part of the constellation of defects identified in Shone's complex, characterized in addition by subaortic obstruction, parachute mitral valve, and supravalvar mitral ring [105].

Pathophysiology

The hemodynamic repercussions of this lesion relate to obstruction of systemic blood flow. The main physiologic consequence being that of increased left ventricular afterload and stroke work. The clinical features of patients with CoA vary relative to the timing of presentation (early versus late). An early presentation is considered that in the neonate/infant, whereas a presentation later in life refers to that in childhood, adolescence or adulthood. In the neonatal period, a clinical picture of hemodynamic instability/shock and ductal dependence for systemic blood flow is consistent with a severe or critical CoA. In this setting an element of ventricular dysfunction is frequently present, in many cases, severe. Infants with CoA typically demonstrate evidence of right ventricular dilation and congestive symptoms. Ductal constriction or lack of patency, within the context of severe aortic narrowing, is associated with arterial hypertension proximal to the site of obstruction and an upper to lower extremity blood pressure gradient. In the older child or adult, the diagnosis may follow evaluation for a murmur, upper extremity hypertension, headache, exercise intolerance or leg fatigue. The progressive development of collateral circulation around the region of CoA is typically found with longstanding pathology. In some cases, particularly with significant collateral development, even in the presence of severe aortic arch obstruction, the patient may remain asymptomatic.

Management Considerations

Because the management options in CoA depend on the anatomical features and the presence of coexistent cardiovascular malformations, no single approach is suitable in all patients [106]. Catheter-based interventions consist of balloon angioplasty with or without stent placement. Surgical strategies have evolved over the years and include subclavian flap repair, patch aortoplasty, resection and end-to-end anastomosis, extended end-to-end repair, and aortic arch advancement. The use of prosthetic material such as interposition grafts or extra-anatomical bypass grafts is less favored today, particularly in young children, because of the need for replacement with somatic growth. The optimal strategy for the treatment of native CoA (balloon angioplasty versus surgery) remains a matter of debate.

The surgical approach to alleviate the obstruction in most cases involves a lateral thoracotomy or median sternotomy, depending on the anatomic details and the planned procedure. In regards to the timing of surgery, early interventions are undertaken in neonates with critical disease and more likely in those with associated aortic arch hypoplasia and symptomatic infants; elective procedures are considered in patients with CoA encountered later in life.

Applications of Transesophageal Echocardiography

It is rare that TEE is required for evaluation of an isolated CoA. Imaging modalities such as TTE, MRI, CT, and cardiac catheterization/angiography are better suited to define the site, extent of the aortic narrowing, and severity of obstruction than is TEE. Several case reports have documented the use of TEE in the assessment of CoA; most of these data have been in reference to the adult patient [107–109]. The limited experience indicates that 2D TEE assisted by color and spectral Doppler can aid in the identification and characterization of CoA. Although TEE has been able to recognize some complications related to the native pathology [110] or treatment [111], it has significant limitations [112]. The approaches to this pathology in the cardiac catheterization laboratory are guided by fluoroscopy and angiography; thus, the use of TEE is unlikely in this setting.

Depending upon the surgical approach (thoracotomy versus sternotomy) and the need to address associated defects, TEE may be considered in the patient undergoing CoA repair. If a thoracotomy is planned, TEE rarely is necessary and, if so, its indication is primarily to evaluate ventricular function during the aortic cross-clamp application; however, even then the need for TEE would be unusual. On occasion, if concerns remain regarding the intracardiac anatomy, a TEE examination might be undertaken in the operating room prior to a planned thoracotomy procedure; once the study is completed, the imaging probe often is removed.

If the intervention is performed via a median sternotomy approach, TEE can be used whether the planned intervention is solely to address the CoA or also to repair associated defects. In the former setting, the primary goal of TEE is intraoperative monitoring and, in some cases, reevaluation of the anatomy and hemodynamics of left-sided structures once the distal aortic arch obstruction has been relieved and the ductus has been ligated. If surgery is also undertaken to repair coexistent anomalies, TEE can be applied to the prebypass and postbypass assessments, particularly for ensuring the adequacy of the intervention(s) and for intraoperative monitoring.

The long-term surveillance of complications related to native pathology, residual disease, or problems as a result of catheter or surgical interventions requires imaging modalities other than TEE [113].

Goals of TEE Prior to Surgical Intervention

Evaluation of CoA

As previously noted, despite the limitations of TEE, this modality has been applied in the evaluation of CoA in adult patients. Anatomic and hemodynamic information may be obtained by a combination of multiple planes that display the aorta in long and short axis views [108, 114]. This examination is accomplished by rotating the imaging probe posteriorly behind the heart and advancing the transducer from the upper esophagus to mid esophageal levels. Pertinent cross-sections include the UE Ao Arch SAX, upper esophageal aortic arch long axis (UE Ao Arch LAX), and ME Desc Ao SAX and LAX views (Fig. 13.28, Video 13.17). Sweeps of the TEE imaging probe are also helpful to delineate the anatomy (Fig. 13.29, Video 13.18). Color flow mapping of the descending aorta can display aliasing in the affected region of the thoracic aorta, or identify turbulent, high velocity jets around the area of obstruction. Changes in these flow patterns can be confirmed after the repair is completed. Continuous flow from collateral vessels may also be identified in this region.

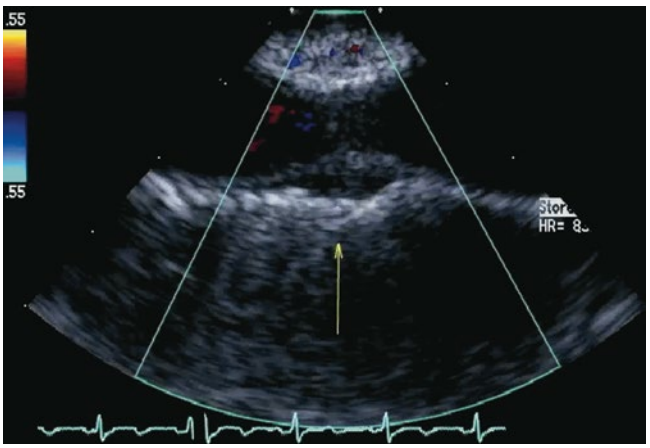

Fig. 13.28 Coarctation of the aorta. Mid esophageal descending aorta long axis view depicting narrowing at the level of the thoracic descending aorta (*arrow*) (Reproduced with permission from Russell et al. [131])

Although optimal alignment of the Doppler beam with the direction of blood flow may not be feasible, precluding an accurate estimation of a peak instantaneous pressure gradient across this region by the simplified Bernoulli equation ($\Delta P = 4V^2$, V = velocity in meters per second), flow acceleration may be detected in this region. A pressure gradient can be obtained across the area of narrowing, with an antegrade spectral flow pattern that extends into diastole, with increasing severity of the obstruction [107]. Blunting of the arterial systolic upstroke and a delay in the mean acceleration rate can also be detected by sampling the descending aorta using the Desc Ao LAX at the level of the abdomen. In some infants a similar evaluation might on occasion be possible using the deep transgastric approach by sampling descending aortic flow at or below the level of the diaphragm.

Characterization and Hemodynamic Assessment of Associated Defects

TEE also can be beneficial in the morphologic and hemodynamic assessment of associated lesions such as a bicuspid aortic valve, ventricular septal defect, left ventricular outflow, or inflow-related pathology [115]. The particular views of interest are dictated by the specific anatomic abnormalities. The reader is referred to other chapters in this textbook that specifically focus on each of the associated pathologies.

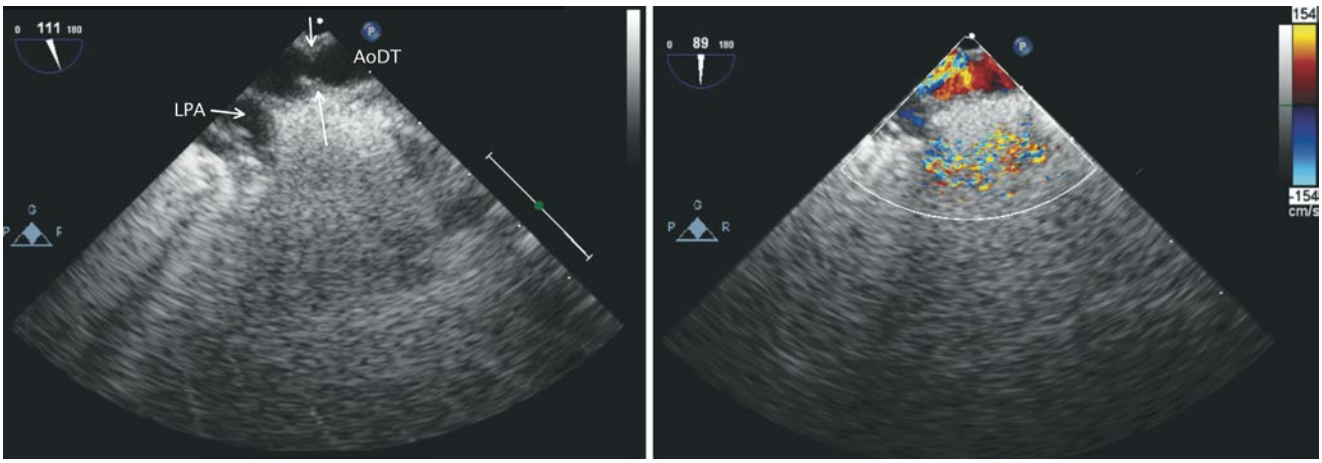

Fig. 13.29 Coarctation of the aorta. *Left panel*, upper esophageal aortic arch short axis view with leftwards transducer rotation demonstrating the descending aorta (*AoDT*) displayed longitudinally as well as the left pulmonary artery (*LPA*). A discrete area of narrowing is noted (*arrows*) corresponding to the area of aortic obstruction. *Right panel*, color Doppler imaging displays turbulent flow across the region of obstruction. These images were obtained in an infant with a ductal-dependent coarctation

Additional Applications

TEE in this setting allows for intraoperative monitoring, evaluation of the left ventricular size and function, estimation of pulmonary artery pressure, and identification of additional anatomic and hemodynamic abnormalities.

Goals of TEE After Surgical Intervention

Postsurgical Assessment

As with the other congenital malformations discussed throughout this textbook, TEE plays an important role in the assessment of the surgical repair, serving to evaluate any hemodynamically significant residual pathology. This should be the focus of the examination. As previously noted, TEE is usually unnecessary for evaluation of aortic arch obstruction alone. However, in postoperative patients with CoA in whom a TEE is performed for evaluation of associated defects, the aortic arch and descending aorta can be investigated both by 2D imaging and color flow Doppler, using TEE views similar to those used in the preoperative evaluation. While these views are not always optimal, they can sometimes provide useful information about the status of the aortic arch/coarctation repair.

Interrupted Aortic Arch

Anatomic Features

Interrupted aortic arch (IAA) is characterized by discontinuity between the proximal and distal segments of the aortic arch. This defect is relatively rare, accounting for less than 1.5 % of all congenital heart defects. The malformation was once thought to result from altered fetal hemodynamics and consequent abnormal development of the aortic arch [116]. The fact that IAA is seen in children with DiGeorge syndrome and related conditions associated with deletions of the chromosome 22q11 [117] has brought into question the theory of fetal hemodynamics and suggested a genetic etiology.

The site of interruption is variable, and as classified by Celoria and Patton [118], may occur at any of three levels as follows (Fig. 13.30):

- In *type A*, the interruption occurs distal to the left subclavian artery at the aortic isthmus. In this case, all the aortic arch vessels are proximal to the interruption, and blood flow in the descending aorta depends on ductal patency. A severe form of aortic coarctation resembles this lesion.
- In *type B*, the interruption occurs at the distal aortic arch between the left common carotid artery and left subclavian artery. It is the most common type of IAA and the one associated with DiGeorge syndrome (at least 15 % of patients).
- In *type C*, the interruption takes place in the proximal aortic arch between the innominate artery (brachiocephalic trunk) and left common carotid artery. This type is quite rare.

Associated Defects

Regardless of the type of interruption, IAA defects are *always* ductal-dependent lesions, thus ductal patency is

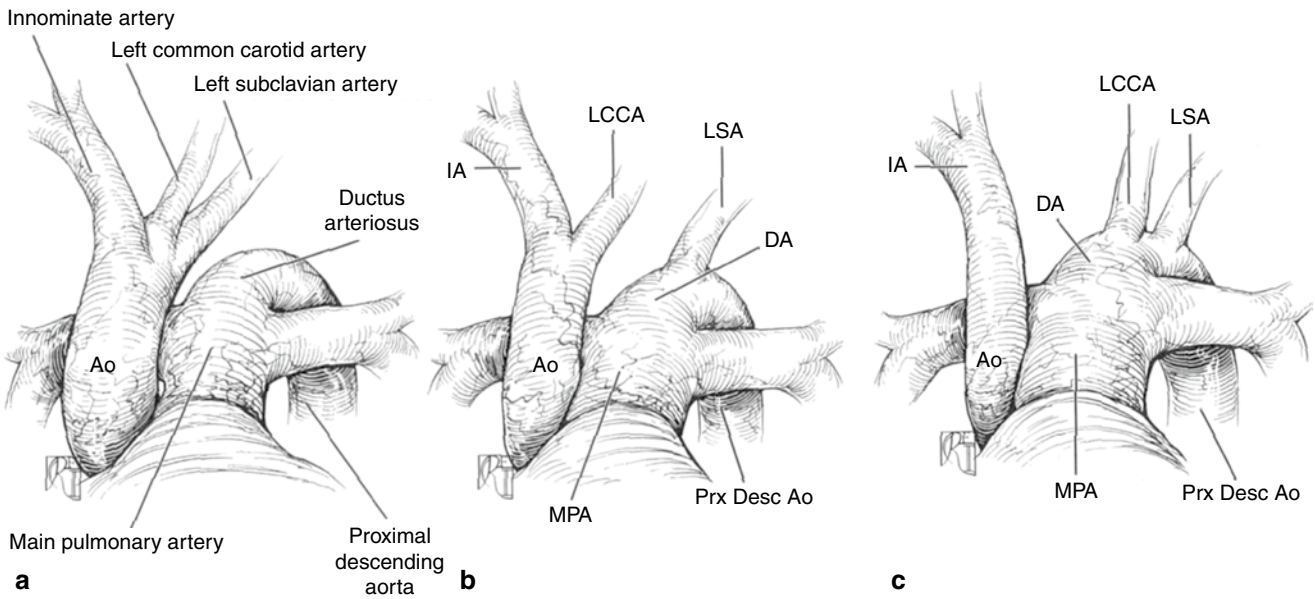

Fig. 13.30 Interrupted aortic arch. Graphic depiction of the various anatomic types of interrupted aortic arch, as described by Celoria and Patton. (**a**) *Type A*, interruption distal to the left subclavian artery. (**b**) *Type B*, interruption between the left carotid and left subclavian arteries. (**c**) *Type C*, interruption between the innominate and left carotid arteries. *Ao* aorta, *DA* ductus arteriosus, *IA* innominate artery, *LCCA* left common carotid artery, *LSA* left subclavian artery, *MPA* main pulmonary artery, *Prx Desc Ao* proximal descending aorta (Reproduced with permission from Jonas [136])

required for perfusion of the descending aorta and any accompanying head and neck vessels arising from the descending aorta. IAA is almost always associated with other intracardiac anomalies such as a ventricular septal defect and subaortic stenosis [119]. A significant number of patients (over 80 %) will have a concomitant ventricular septal defect; this defect is typically large and unrestrictive. The characterization of the ventricular septal defect in this lesion is that of a 'malalignment-type' of defect; the conal (infundibular) or outlet muscular septum is posteriorly deviated relative to the remaining ventricular septum, leading to crowding of the left ventricular outflow tract and resultant variable degrees of subaortic obstruction. It may be present within the context of a bicuspid aortic valve, as well as hypoplasia of the aortic annulus and root. Other important associated lesions include truncus arteriosus, AP, double outlet right ventricle, transposition of the great arteries, and single ventricle malformations. In many of these associated defects, IAA is frequently seen within the context of narrowing or stenosis of the aortic outflow tract; thus the finding of aortic tract narrowing should always prompt a search for arch obstruction/interruption.

An aberrant subclavian artery (arising from the descending thoracic aorta, distal to the PDA) represents a frequent finding in IAA, occurring in approximately 25–30 % of cases [120]. Aortic arch sidedness anomalies can also be seen. In the setting of a left aortic arch, an aberrant subclavian artery, if present, originates distal to the site of interruption as the last vessel (anomalous right subclavian artery). In a right aortic arch, the anomalous subclavian, if present, is the left subclavian artery.

Pathophysiology

The clinical presentation of IAA typically is in the first few days of life. The scenario varies but usually is that of a neonate with respiratory distress, heart failure, cyanosis, or poor cardiac output and impending or overt cardiovascular collapse. Cardiovascular decompensation is the result of ductal closure leading to hypoperfusion of major organs and vascular beds distal to the obstruction. Without treatment, such patients generally expire soon after presentation. Intravenous prostaglandin E_1 therapy is usually necessary to maintain systemic blood flow. In very rare cases, the ductus arteriosus fails to close and patients can survive (clinically undetected) into childhood or beyond.

Management Considerations

The definitive surgical management of this lesion consists of arch reconstruction, at which time associated defects also are addressed [121]. In the current surgical area, the preferred approach is that of a single-stage procedure in the neonate in which aortic continuity is established by end-to-end anastomosis of the proximal and distal arch segments [122, 123]. Patch closure of the ventricular septal defect is accomplished via a transatrial or transpulmonary approach. Depending on the severity of the obstruction, interventions may be required to enlarge the left ventricular outflow tract. This is usually performed by resection of the muscular outlet septum. However in some instances more extensive surgery, such as a Konno-type procedure, Yasui procedure or aortic root replacement, might be necessary to alleviate the subaortic obstruction and/or aortic root hypoplasia [122]. In some patients, the anatomy is not suitable for a biventricular approach and a single ventricle strategy must be undertaken.

Late issues that can lead to morbidity and in some cases require reintervention include outflow tract problems, aortic arch obstruction, and residual intracardiac shunts.

Applications of Transesophageal Echocardiography

In almost all neonates with IAA, TTE provides accurate diagnosis and definition of the anatomic abnormalities, and is sufficient for surgical planning. Occasionally, additional imaging in the form of MRI or chest CT is performed to further delineate the anatomy, particularly details of extracardiac structures such as the aortic arch (sidedness, aberrant subclavian artery, and site of interruption) or associated anomalies [124]. As such, TEE is rarely used strictly for diagnostic evaluation of the great artery abnormalities. However, as is the case with many of the other congenital heart defects discussed in this chapter and throughout this textbook, TEE still plays a significant role in the perioperative setting. Although TEE has limited utility for the assessment of the aortic arch and its reconstruction, it is extremely helpful in the evaluation of the pathologies frequently associated with IAA. These are discussed below.

Goals of TEE Prior to Surgical Intervention

Characterization of the Ventricular Septal Defect

The interventricular communication should be defined in terms of size, location, flow direction, and velocity. In addition, the presence of additional ventricular septal defects should be considered. The approach described in detail in Chap. 9 for the comprehensive evaluation of the ventricular septum is recommended. Particular cross-sections of interest are those allowed by the ME 4 Ch, ME AV SAX, and ME LAX views. The orientation of the outlet septum with respect to the trabecular interventricular septum should be explored to evaluate for potential posterior septal malalignment and concomitant subaortic obstruction. TEE views that allow for this assessment include the ME 4 Ch with probe anteflexion to bring the aorta into view, ME LAX, ME AV LAX, transgastric long axis (TG LAX), and DTG LAX, and DTG Sagittal views (Figs. 13.31, 13.32, and 13.33; Videos 13.19, 13.20, and 13.21). Multiple

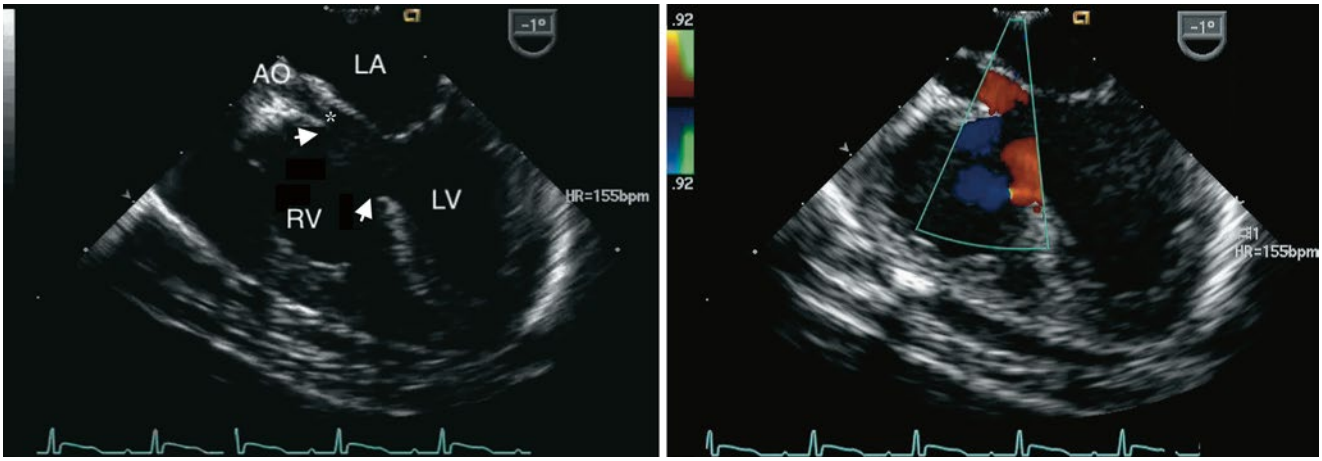

Fig. 13.31 Interrupted aortic arch. Two-dimensional mid esophageal four chamber image (*left panel*) and corresponding color flow mapping (*right panel*) in an infant with interrupted aortic arch demonstrating a large posteriorly malaligned ventricular septal defect as marked by the *arrowheads*. The hypoplastic subaortic region and aortic annulus are also shown (*asterisk*). *AO* aorta, *LA* left atrium, *LV* left ventricle, *RV* right ventricle

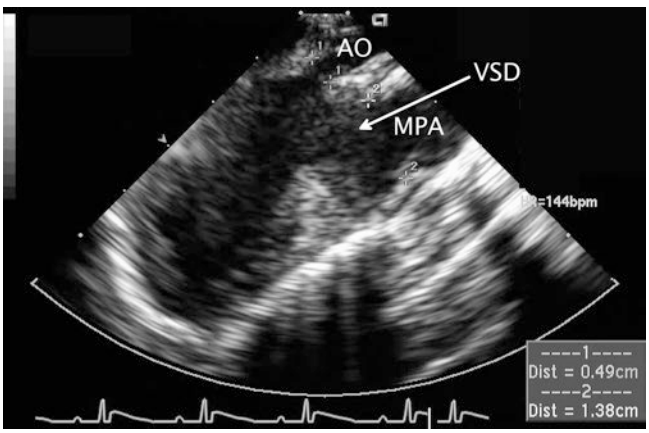

Fig. 13.32 Interrupted aortic arch. Mid esophageal aortic valve long axis view obtained from the same infant as shown in Fig. 13.31, demonstrating the ventricular septal defect (*VSD*) and marked discrepancy in the sizes of the arterial roots. *AO* aorta, *MPA* main pulmonary artery

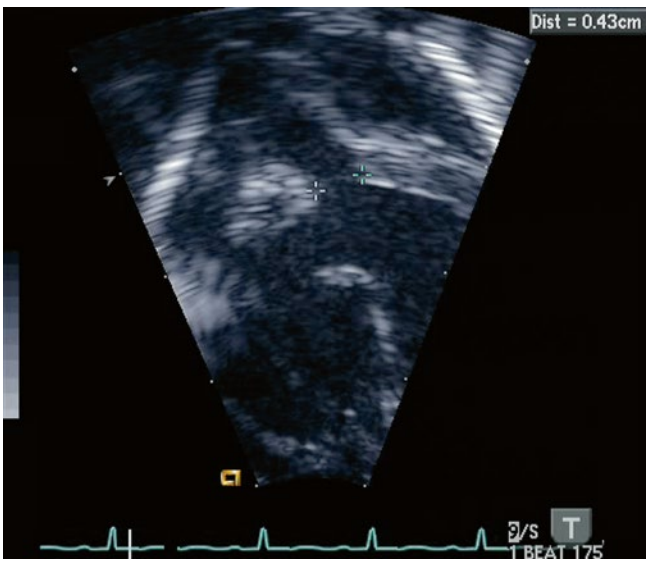

Fig. 13.33 Interrupted aortic arch. Deep transgastric long axis image from infant with interrupted aortic arch demonstrating the ventricular septal defect and subaortic narrowing. The figure indicates measurement of the aortic annulus

sweeps of the ventricular septum are suggested to evaluate the anatomy fully.

Characterization of the Subaortic Region

The left ventricular outflow tract should be fully characterized in terms of size, nature of flow (laminar versus turbulent), and patency. This is best accomplished by a combination of mid esophageal (ME AV LAX, ME LAX) and deep transgastric imaging (Figs. 13.32 and 13.33; Videos 13.20 and 13.21). Doppler interrogation (both pulsed and continuous wave Doppler) should be applied to define the level and severity of an obstruction, if present. The deep transgastric windows provide an optimal angle for spectral Doppler interrogation (Fig. 13.34). This evaluation should include determination of peak and mean velocities for estimation of peak and mean gradients. A caveat to be considered is that flow velocities may underestimate the severity of the obstruction due to: (1) reduced prograde flow across these structures related to the interruption, (2) the presence of left-to-right shunting across the ventricular septal defect, and (3) associated impaired ventricular systolic function. Detailed measurements of the subaortic region, aortic valve annulus, and root should be obtained in multiple views, as this information can impact the surgical intervention and dictate the need for more complex procedures as previously noted (Figs. 13.32 and 13.33). In addition, the information can help to predict left ventricular outflow obstruction after repair of the defect. Parameters that may determine either the likelihood of

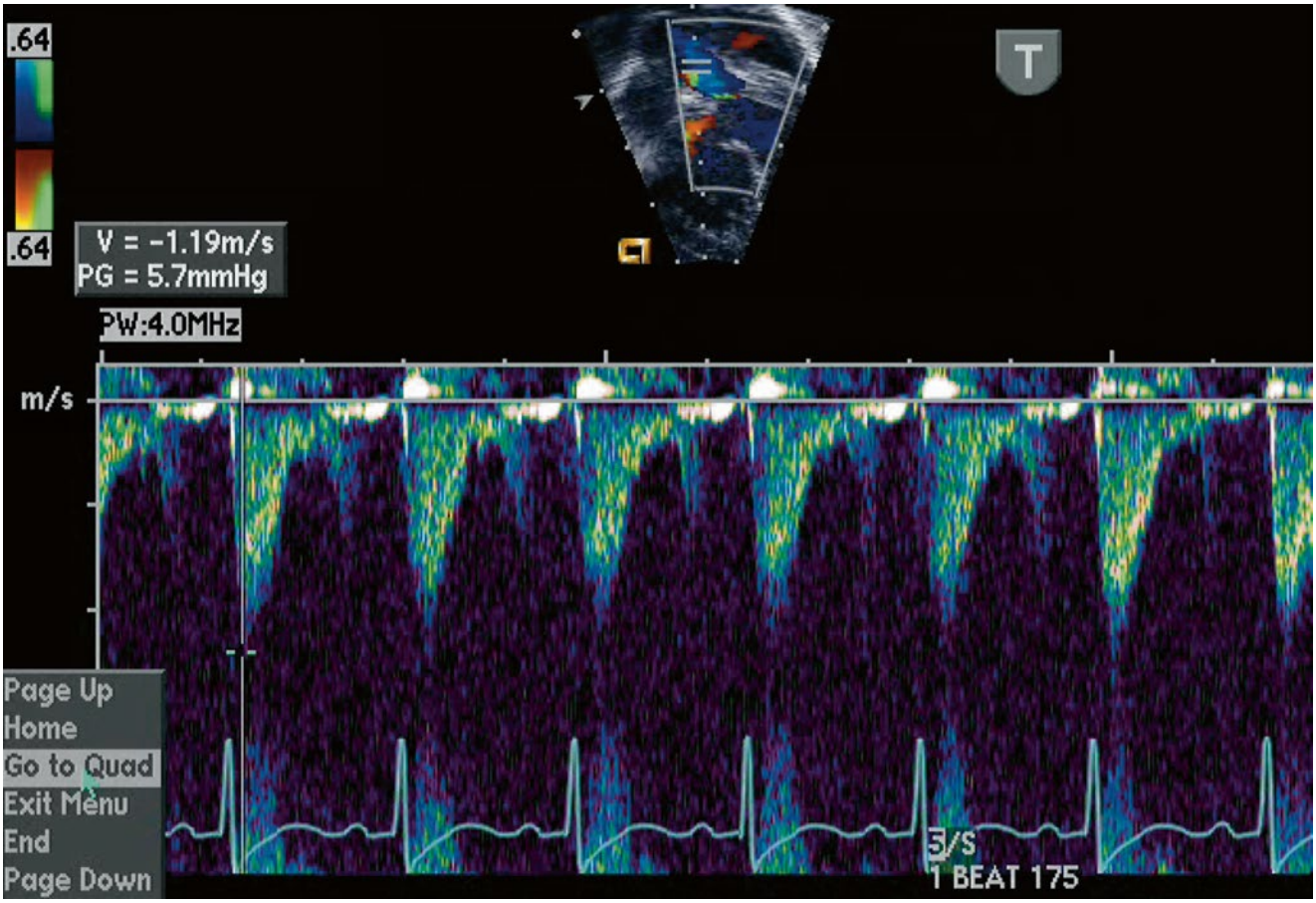

Fig. 13.34 Interrupted aortic arch. Spectral Doppler tracing obtained in the deep transgastric window across the left ventricular outflow tact corresponding to the patient depicted in Fig. 13.33

postoperative subaortic obstruction in IAA (left ventricular outflow tract area <0.7 cm/m^2) or need for a single ventricle strategy (subaortic diameter <3 mm) have been derived from preoperative TTE imaging [125–128]. TEE allows for these measurements to be confirmed and provides further information that could influence the surgical options or predict long-term outcome.

Characterization of the Aortic Valve

The aortic valve should be evaluated to determine morphology, number of cusps, mobility, and competence. The ME AV SAX and LAX, as well as the ME RV In-Out view, are particularly suited for this evaluation. The ME Asc Ao SAX (Video 13.22) and LAX views facilitates the assessment of the ascending aorta. Although pulsed and continuous Doppler analysis allow for determination of flow velocities across the aortic valve, the potentially associated subvalvar narrowing and the presence of an adjacent ventricular septal defect may render this evaluation challenging. As previously noted, these factors could interfere with the assessment of the separate contributions of annular size or concomitant valve pathology to the outflow obstruction. Thus, to a great extent, this determination is qualitative in nature and based primarily on morphologic findings as demonstrated by 2D imaging.

Additional Applications

The prebypass evaluation should include examination of the atrial septum for the presence of a communication, assessment of atrioventricular valve morphology and flows, and baseline determination of ventricular systolic function.

Goals of TEE After Surgical Intervention

Detection of Residual Intracardiac Shunts

The postoperative TEE examination should include 2D and Doppler interrogation for residual VSD patch leaks or other residual shunts at either the atrial or ventricular level (Fig. 13.35, Videos 13.23 and 13.24). The size and direction of blood flow across the communication, as well as hemodynamic significance of any residual intracardiac defect, should be ascertained. The same TEE views described in the preoperative examination should be utilized.

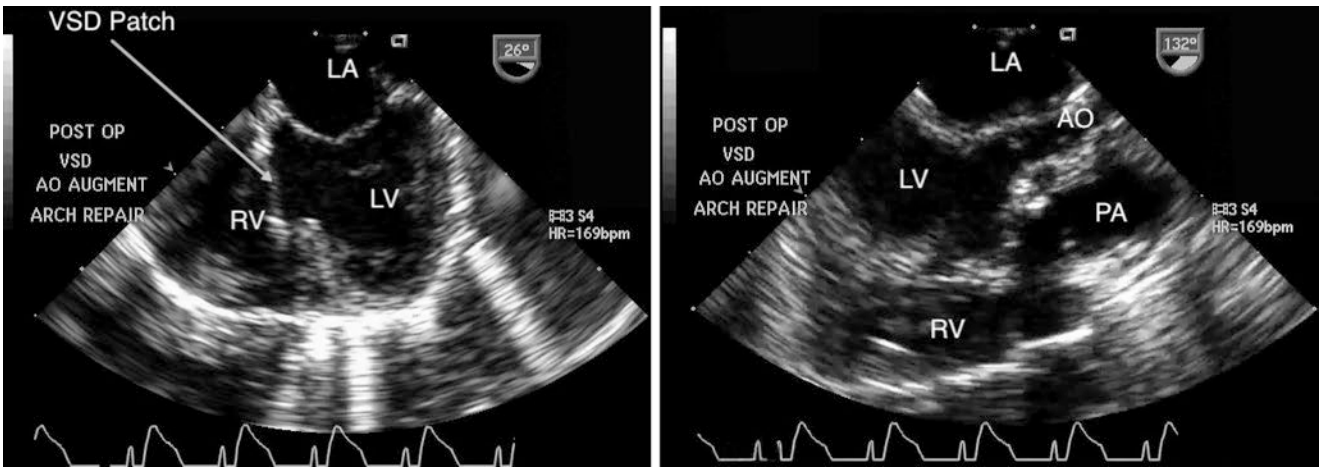

Fig. 13.35 Interrupted aortic arch. Intraoperative images in orthogonal planes (*left* and *right panels*) obtained following aortic arch advancement, subaortic resection, and ventricular septal defect closure in the infant with interrupted aortic arch shown in Figs. 13.31 and 13.32. Note the large pericardial patch across the ventricular septal defect (*VSD patch*) and the relatively small subaortic area, aortic annulus, and aortic root. *AO* aorta, *LA* left ventricle, *LV* left ventricle, *PA* main pulmonary artery, *RV* right ventricle

Assessment of Residual Subaortic Obstruction

In all patients, and particularly in those with concerns regarding left ventricular outflow tract obstruction, a comprehensive multiplane TEE examination should be undertaken after the surgical repair. The same approach applies to the patient undergoing reintervention for residual or recurrent subaortic obstruction in the prebypass and postbypass settings. It is imperative to assess the severity of the left ventricular outflow tract obstruction by both qualitative and quantitative methods (Videos 13.23 and 13.24). The same TEE views used for preoperative 2D evaluation of the subaortic region, and for optimal Doppler assessment, should also be used postoperatively to facilitate this interrogation.

Aortic Arch Evaluation

As with CoA surgery, in some cases portions of the aortic arch and descending aorta can be visualized both by 2D imaging color flow Doppler, using a combination of upper and mid esophageal TEE views (outlined in the CoA section above). Again, while these views are not optimal, they can sometimes provide useful information about the status of the aortic arch repair.

Additional Applications

In the postbypass examination, atrioventricular valve competence and systolic ventricular function should be examined and compared to the preoperative findings (Video 13.25). Patch closure of the VSD may require a radial incision along the tricuspid valve annulus to enhance surgical exposure of the defect. Although on follow-up this intervention has not been associated with tricuspid valve dysfunction [129], the postoperative TEE should evaluate flow across the tricuspid valve to ensure the absence of obstruction and/or regurgitation, or any other changes from the baseline examination. The follow-up assessment and long-term surveillance of aortic arch reconstruction requires modalities other than TEE to exclude recurrent obstruction.

Summary

Congenital anomalies that affect the great arteries and related vascular structures are identified and well defined by noninvasive imaging modalities. High-resolution transthoracic imaging represents the initial, and often the sole, diagnostic approach required to outline medical and surgical management plans in affected patients. In view of limitations related to the TEE imaging approach, which in some cases will not allow adequate or comprehensive definition of vascular structures, the diagnostic role of this modality can be somewhat limited. However, this does not negate the value of TEE in such patients. In the intraoperative setting, TEE may still be able to confirm the presence of abnormal vascular structure(s) or connection(s). Frequently, the malformations that affect the great arteries are associated with coexistent pathology, and not uncommonly these malformations are of a complex nature. TEE facilitates the detailed evaluation of these defects in terms of anatomic and hemodynamic assessment while playing a major role in surgical planning. This imaging modality also provides for intraoperative monitoring, assessment of the adequacy of the surgical intervention(s), and guidance of the revision if required. As such, TEE can provide significant contributions in patients with great artery and other vascular anomalies.

References

1. Knight L, Edwards JE. Right aortic arch. Types and associated cardiac anomalies. Circulation. 1974;50:1047–51.
2. Mugge A, Daniel WG, Lichtlen PR. Imaging of patent ductus arteriosus by transesophageal color-coded Doppler echocardiography. J Clin Ultrasound. 1991;19:128–9.
3. Szulc M, Ritter SB. Patent ductus arteriosus in an infant with atrioventricular septal defect and pulmonary hypertension: diagnosis by transesophageal color flow echocardiography. J Am Soc Echocardiogr. 1991;4:194–8.
4. Takenaka K, Sakamoto T, Shiota T, et al. Diagnosis of patent ductus arteriosus in adults by biplane transesophageal color Doppler flow mapping. Am J Cardiol. 1991;68:691–3.
5. Shyu KG, Lai LP, Lin SC, et al. Diagnostic accuracy of transesophageal echocardiography for detecting patent ductus arteriosus in adolescents and adults. Chest. 1995;108:1201–5.
6. Andrade A, Vargas-Barron J, Rijlaarsdam M, et al. Utility of transesophageal echocardiography in the examination of adult patients with patent ductus arteriosus. Am Heart J. 1995;130:543–6.
7. Krauss D, Weinert L, Lang RM. The role of multiplane transesophageal echocardiography in diagnosing PDA in an adult. Echocardiography. 1996;13:95–8.
8. Chang ST, Hung KC, Hsieh IC, et al. Evaluation of shunt flow by multiplane transesophageal echocardiography in adult patients with isolated patent ductus arteriosus. J Am Soc Echocardiogr. 2002;15:1367–73.
9. Tumbarello R, Sanna A, Cardu G, et al. Usefulness of transesophageal echocardiography in the pediatric catheterization laboratory. Am J Cardiol. 1993;71:1321–5.
10. Chuang YC, Yin WH, Hsiung MC, et al. Successful transcatheter closure of a residual patent ductus arteriosus with complex anatomy after surgical ligation using an amplatzer ductal occluder guided by live three-dimensional transesophageal echocardiography. Echocardiography. 2011;28:E101–3.
11. Marek T, Zelizko M, Kautzner J. Images in cardiovascular medicine. Real-time 3-dimensional transesophageal echocardiography imaging: adult patent ductus arteriosus before and after transcatheter closure. Circulation. 2009;120:e92–3.
12. Wang KY, Hsieh KS, Yang MW, et al. The use of transesophageal echocardiography to evaluate the effectiveness of patent ductus arteriosus ligation. Echocardiography. 1993;10:53–7.
13. Lavoie J, Burrows FA, Gentles TL, et al. Transoesophageal echocardiography detects residual ductal flow during video-assisted thoracoscopic patent ductus arteriosus interruption. Can J Anaesth. 1994;41:310–3.
14. Lavoie J, Javorski JJ, Donahue K, et al. Detection of residual flow by transesophageal echocardiography during video-assisted thoracoscopic patent ductus arteriosus interruption. Anesth Analg. 1995;80:1071–5.
15. Shiota T, Omoto R, Cobanoglu A, et al. Usefulness of transesophageal imaging of flow convergence region in the operating room for evaluating isolated patent ductus arteriosus. Am J Cardiol. 1997;80:1108–12.
16. Ho AC, Tan PP, Yang MW, et al. The use of multiplane transesophageal echocardiography to evaluate residual patent ductus arteriosus during video-assisted thoracoscopy in adults. Surg Endosc. 1999;13:975–9.
17. Hatle L, Anglesen B. Pulsed and continuous wave Doppler in diagnosis and assessment of various heart lesions. In: Hatle L, Anglesen B, editors. Doppler ultrasound in cardiology. Physical principles and clinical applications. Philadelphia: Lea & Febiger; 1985. p. 97–292.
18. Hiraishi S, Horiguchi Y, Misawa H, et al. Noninvasive Doppler echocardiographic evaluation of shunt flow dynamics of the ductus arteriosus. Circulation. 1987;75:1146–53.
19. Cloez JL, Isaaz K, Pernot C. Pulsed Doppler flow characteristics of ductus arteriosus in infants with associated congenital anomalies of the heart or great arteries. Am J Cardiol. 1986;57:845–51.
20. Shiraishi H, Yanagisawa M. Bidirectional flow through the ductus arteriosus in normal newborns: evaluation by Doppler color flow imaging. Pediatr Cardiol. 1991;12:201–5.
21. Serwer GA, Armstrong BE, Anderson PA. Nonivasive detection of retrograde descending aortic flow in infants using continuous wave doppler ultrasonography. Implications for diagnosis of aortic runoff lesions. J Pediatr. 1980;97:394–400.
22. Musewe NN, Smallhorn JF, Benson LN, et al. Validation of Doppler-derived pulmonary arterial pressure in patients with ductus arteriosus under different hemodynamic states. Circulation. 1987;76:1081–91.
23. Snider AR. The ductus arteriosus: a window for assessment of pulmonary artery pressures? J Am Coll Cardiol. 1990;15:457–8.
24. Marx GR, Allen HD, Goldberg SJ. Doppler echocardiographic estimation of systolic pulmonary artery pressure in patients with aortic-pulmonary shunts. J Am Coll Cardiol. 1986;7:880–5.
25. Milan A, Magnino C, Veglio F. Echocardiographic indexes for the non-invasive evaluation of pulmonary hemodynamics. J Am Soc Echocardiogr. 2010;23:225–39; quiz 332–4.
26. Neufeld HN, Lester RG, Adams PJ, et al. Aorticopulmonary septal defect. Am J Cardiol. 1962;9:12–25.
27. Mori K, Ando M, Takao A, et al. Distal type of aortopulmonary window. Report of 4 cases. Br Heart J. 1978;40:681–9.
28. Kutsche LM, Van Mierop LH. Anatomy and pathogenesis of aorticopulmonary septal defect. Am J Cardiol. 1987;59:443–7.
29. Richardson JV, Doty DB, Rossi NP, et al. The spectrum of anomalies of aortopulmonary septation. J Thorac Cardiovasc Surg. 1979; 78:21–7.
30. Ho SY, Gerlis LM, Anderson C, et al. The morphology of aortopulmonary windows with regard to their classification and morphogenesis. Cardiol Young. 1994;4:146–55.
31. Murin P, Sinzobahamvya N, Blaschczok HC, et al. Aortopulmonary window associated with interrupted aortic arch: report of surgical repair of eight cases and review of literature. Thorac Cardiovasc Surg. 2012;60:215–20.
32. Pace Napoleone C, Oppido G, Angeli E, et al. Aortopulmonary window and anomalous coronary artery: an exceptional association. Ann Thorac Surg. 2011;91:1272–4.
33. Stamato T, Benson LN, Smallhorn JF, et al. Transcatheter closure of an aortopulmonary window with a modified double umbrella occluder system. Cathet Cardiovasc Diagn. 1995;35:165–7.
34. Tulloh RM, Rigby ML. Transcatheter umbrella closure of aortopulmonary window. Heart. 1997;77:479–80.
35. Jureidini SB, Spadaro JJ, Rao PS. Successful transcatheter closure with the buttoned device of aortopulmonary window in an adult. Am J Cardiol. 1998;81:371–2.
36. Srivastava A, Radha AS. Transcatheter closure of a large aortopulmonary window with severe pulmonary arterial hypertension beyond infancy. J Invasive Cardiol. 2012;24:E24–6.
37. Doty DB, Richardson JV, Falkovsky GE, et al. Aortopulmonary septal defect: hemodynamics, angiography, and operation. Ann Thorac Surg. 1981;32:244–50.
38. Hew CC, Bacha EA, Zurakowski D, et al. Optimal surgical approach for repair of aortopulmonary window. Cardiol Young. 2001;11:385–90.
39. Jonas RA. Patent ductus arteriosus, aortopulmonary window, sinus of valsalva fistula, aortoventricular tunnel. In: Jonas RA, editor. Comprehensive surgical management of congenital heart disease. New York: Arnold; 2004. p. 195–9.
40. Rice MJ, Seward JB, Hagler DJ, et al. Visualization of aortopulmonary window by two-dimensional echocardiography. Mayo Clin Proc. 1982;57:482–7.
41. Smallhorn JF, Anderson RH, Macartney FJ. Two dimensional echocardiographic assessment of communications between ascending

aorta and pulmonary trunk or individual pulmonary arteries. Br Heart J. 1982;47:563–72.
42. Lau KC, Calcaterra G, Miller GA, et al. Aorto-pulmonary window. J Cardiovasc Surg (Torino). 1982;23:21–7.
43. Alboliras ET, Chin AJ, Barber G, et al. Detection of aortopulmonary window by pulsed and color Doppler echocardiography. Am Heart J. 1988;115:900–2.
44. Balaji S, Burch M, Sullivan ID. Accuracy of cross-sectional echocardiography in diagnosis of aortopulmonary window. Am J Cardiol. 1991;67:650–3.
45. Mahle WT, Kreeger J, Silverman NH. Echocardiography of the aortopulmonary window, aorto-ventricular tunnels, and aneurysm of the sinuses of Valsalva. Cardiol Young. 2010;20 Suppl 3:100–6.
46. Singh A, Mehmood F, Romp RL, et al. Live/Real time three-dimensional transthoracic echocardiographic assessment of aorto-pulmonary window. Echocardiography. 2008;25:96–9.
47. Samdarshi TE, Morrow WR, Nanda NC, et al. Transesophageal echocardiography in aortopulmonary communications. Echocardiography. 1991;8:383–95.
48. Barnes ME, Mitchell ME, Tweddell JS. Aortopulmonary window. Semin Thorac Cardiovasc Surg Pediatr Card Surg Annu. 2011;14:67–74.
49. Contro S, Miller RA, White H, et al. Bronchial obstruction due to pulmonary artery anomalies. I. Vascular sling. Circulation. 1958; 17:418–23.
50. Castaneda AR. Pulmonary artery sling. Ann Thorac Surg. 1979; 28:210–1.
51. Adam MP, Schelley S, Gallagher R, et al. Clinical features and management issues in Mowat-Wilson syndrome. Am J Med Genet A. 2006;140:2730–41.
52. Strenge S, Heinritz W, Zweier C, et al. Pulmonary artery sling and congenital tracheal stenosis in another patient with Mowat-Wilson syndrome. Am J Med Genet A. 2007;143A:1528–30.
53. Backer CL, Russell HM, Kaushal S, et al. Pulmonary artery sling: current results with cardiopulmonary bypass. J Thorac Cardiovasc Surg. 2012;143:144–51.
54. Newman B, Meza MP, Towbin RB, et al. Left pulmonary artery sling: diagnosis and delineation of associated tracheobronchial anomalies with MR. Pediatr Radiol. 1996;26:661–8.
55. Sade RM, Rosenthal A, Fellows K, et al. Pulmonary artery sling. J Thorac Cardiovasc Surg. 1975;69:333–46.
56. Berdon WE, Baker DH, Wung JT, et al. Complete cartilage-ring tracheal stenosis associated with anomalous left pulmonary artery: the ring-sling complex. Radiology. 1984;152:57–64.
57. Gikonyo BM, Jue KL, Edwards JE. Pulmonary vascular sling: report of seven cases and review of the literature. Pediatr Cardiol. 1989;10:81–9.
58. Binet JP, Longlois J. Aortic arch anomalies in children and infants. J Thorac Cardiovasc Surg. 1977;73:248–52.
59. Backer CL. Vascular rings, slings, and tracheal rings. Mayo Clin Proc. 1993;68:1131–3.
60. Zhong YM, Jaffe RB, Zhu M, et al. CT assessment of tracheobronchial anomaly in left pulmonary artery sling. Pediatr Radiol. 2010;40:1755–62.
61. Backer CL, Mavroudis C, Dunham ME, et al. Pulmonary artery sling: results with median sternotomy, cardiopulmonary bypass, and reimplantation. Ann Thorac Surg. 1999;67:1738–44; discussion 1744–5.
62. Jonas RA, Spevak PJ, McGill T, et al. Pulmonary artery sling: primary repair by tracheal resection in infancy. J Thorac Cardiovasc Surg. 1989;97:548–50.
63. Fiore AC, Brown JW, Weber TR, et al. Surgical treatment of pulmonary artery sling and tracheal stenosis. Ann Thorac Surg. 2005; 79:38–46; discussion 38–46.
64. Oshima Y, Yamaguchi M, Yoshimura N, et al. Management of pulmonary artery sling associated with tracheal stenosis. Ann Thorac Surg. 2008;86:1334–8.
65. Huang SC, Wu ET, Wang CC, et al. Surgical management of pulmonary artery sling: trachea diameter and outcomes with or without tracheoplasty. Pediatr Pulmonol. 2012;47:903–8.
66. McCray P, Grandgeorge S, Smith W, et al. Cine CT diagnosis of pulmonary artery sling. Pediatr Radiol. 1986;16:508–10.
67. Yeager SB, Chin AJ, Sanders SP. Two-dimensional echocardiographic diagnosis of pulmonary artery sling in infancy. J Am Coll Cardiol. 1986;7:625–9.
68. Gnanapragasam JP, Houston AB, Jamieson MP. Pulmonary artery sling: definitive diagnosis by colour Doppler flow mapping avoiding cardiac catheterisation. Br Heart J. 1990;63:251–2.
69. Murdison KA, Andrews BA, Chin AJ. Ultrasonographic display of complex vascular rings. J Am Coll Cardiol. 1990;15:1645–53.
70. Lillehei CW, Colan S. Echocardiography in the preoperative evaluation of vascular rings. J Pediatr Surg. 1992;27:1118–20; discussion 1120–1.
71. van Son JA, Julsrud PR, Hagler DJ, et al. Imaging strategies for vascular rings. Ann Thorac Surg. 1994;57:604–10.
72. Backer CL. Diagnostic issues and indications for surgery in patients with pulmonary artery sling. Circulation. 1998;98:188–9.
73. Lee KH, Yoon CS, Choe KO, et al. Use of imaging for assessing anatomical relationships of tracheobronchial anomalies associated with left pulmonary artery sling. Pediatr Radiol. 2001;31:269–78.
74. Newman B, Cho Y. Left pulmonary artery sling—anatomy and imaging. Semin Ultrasound CT MR. 2010;31:158–70.
75. Erickson LC, Cocalis MW, George L. Partial anomalous left pulmonary artery: new evidence on the development of the pulmonary artery sling. Pediatr Cardiol. 1996;17:319–21.
76. Tateishi A, Kawada M. Partial form of a pulmonary artery sling. Ann Thorac Surg. 2009;87:965.
77. Nakajima H, Satomi G, Nakazawa M, et al. Color Doppler and transesophageal echocardiography of vascular sling. Heart Vessels. 1992;7:99–103.
78. Lin CR, Tsai SK, Wang MJ, et al. Airway management and transesophageal echocardiographic monitoring for pulmonary artery sling. J Formos Med Assoc. 1999;98:863–5.
79. Kutsche LM, Van Mierop LH. Anomalous origin of a pulmonary artery from the ascending aorta: associated anomalies and pathogenesis. Am J Cardiol. 1988;61:850–6.
80. Edasery B, Sharma M, Vaddigiri V, et al. Hemitruncus presenting in an adult. A case report. Angiology. 1996;47:1023–6.
81. Aru GM, English WP, Gaymes CH, et al. Origin of the left pulmonary artery from the aorta: embryologic considerations. Ann Thorac Surg. 2001;71:1008–10.
82. Nakamura Y, Yasui H, Kado H, et al. Anomalous origin of the right pulmonary artery from the ascending aorta. Ann Thorac Surg. 1991;52:1285–91.
83. Sotomora RF, Edwards JE. Anatomic identification of so-called absent pulmonary artery. Circulation. 1978;57:624–33.
84. Wu QY, Yang XB. Anomalous origin of the pulmonary artery from the right coronary artery. Ann Thorac Surg. 2001;72:1396–8.
85. Presbitero P, Bull C, Haworth SG, et al. Absent or occult pulmonary artery. Br Heart J. 1984;52:178–85.
86. McCaffrey F. Around pediheart: absent pulmonary artery. Pediatr Cardiol. 2001;22:332.
87. Pfefferkorn JR, Loser H, Pech G, et al. Absent pulmonary artery. A hint to its embryogenesis. Pediatr Cardiol. 1982;3:283–6.
88. Apostolopoulou SC, Kelekis NL, Brountzos EN, et al. "Absent" pulmonary artery in one adult and five pediatric patients: imaging, embryology, and therapeutic implications. AJR Am J Roentgenol. 2002;179:1253–60.
89. Apostolopoulou SC, Kelekis NL. Anomalous origin of pulmonary artery from the innominate artery. Pediatr Cardiol. 2004;25:565.
90. Prifti E, Bonacchi M, Murzi B, et al. Anomalous origin of the left pulmonary artery from the aorta. Our experience and literature review. Heart Vessels. 2003;18:79–84.

91. Peng EW, Shanmugam G, Macarthur KJ, et al. Ascending aortic origin of a branch pulmonary artery—surgical management and long-term outcome. Eur J Cardiothorac Surg. 2004;26:762–6.
92. Morgan JR. Left pulmonary artery from ascending aorta in tetralogy of Fallot. Circulation. 1972;45:653–7.
93. Fontana GP, Spach MS, Effmann EL, et al. Origin of the right pulmonary artery from the ascending aorta. Ann Surg. 1987;206:102–13.
94. Santos MA, Azevedo VM. Anomalous origin of a pulmonary artery from the ascending aorta: surgical repair resolving pulmonary arterial hypertension. Arq Bras Cardiol. 2004;83(503–7):498–502.
95. Fong LV, Anderson RH, Siewers RD, et al. Anomalous origin of one pulmonary artery from the ascending aorta: a review of echocardiographic, catheter, and morphological features. Br Heart J. 1989;62:389–95.
96. Penkoske PA, Castaneda AR, Fyler DC, et al. Origin of pulmonary artery branch from ascending aorta. Primary surgical repair in infancy. J Thorac Cardiovasc Surg. 1983;85:537–45.
97. Mee RB. Surgical repair of hemitruncus: principles and techniques. J Card Surg. 1987;2:247–56.
98. Nathan M, Rimmer D, Piercey G, et al. Early repair of hemitruncus: excellent early and late outcomes. J Thorac Cardiovasc Surg. 2007;133:1329–35.
99. Prifti E, Bonacchi M, Murzi B, et al. Anomalous origin of the right pulmonary artery from the ascending aorta. J Card Surg. 2004;19:103–12.
100. Ishizawa E, Horiuchi T, Tadokoro M, et al. Diagnosis and surgical treatment of "angiographically absent pulmonary artery syndrome". Tohoku J Exp Med. 1978;125:1–9.
101. Moreno-Cabral RJ, McNamara JJ, Reddy VJ, et al. Unilateral absent pulmonary artery: surgical repair with a new technique. J Thorac Cardiovasc Surg. 1991;102:463–5.
102. Duncan WJ, Freedom RM, Olley PM, et al. Two-dimensional echocardiographic identification of hemitruncus: anomalous origin of one pulmonary artery from ascending aorta with the other pulmonary artery arising normally from right ventricle. Am Heart J. 1981;102:892–6.
103. Warnes CA. Bicuspid aortic valve and coarctation: two villains part of a diffuse problem. Heart. 2003;89:965–6.
104. Connolly HM, Jr H, Brown RDJ, et al. Intracranial aneurysms in patients with coarctation of the aorta: a prospective magnetic resonance angiographic study of 100 patients. Mayo Clin Proc. 2003;78:1491–9.
105. Shone JD, Sellers RD, Anderson RC, et al. The developmental complex of "parachute mitral valve," supravalvular ring of left atrium, subaortic stenosis, and coarctation of aorta. Am J Cardiol. 1963;11:714–25.
106. Kenny D, Hijazi ZM. Coarctation of the aorta: from fetal life to adulthood. Cardiol J. 2011;18:487–95.
107. Duffy CI, Plehn JF. Transesophageal echocardiographic assessment of aortic coarctation using color, flow-directed Doppler sampling. Chest. 1994;105:286–8.
108. Engvall J, Sjoqvist L, Nylander E, et al. Biplane transoesophageal echocardiography, transthoracic Doppler, and magnetic resonance imaging in the assessment of coarctation of the aorta. Eur Heart J. 1995;16:1399–409.
109. Trehan VK, Bhardwaj S, Rastogi P, et al. Multiplane transoesophageal echocardiography in an adult with coarctation of aorta. Indian Heart J. 1996;48:707–9.
110. Skinner JR, Bexton R, Wren C. Aortic coarctation endarteritis and aneurysm: diagnosis by transoesophageal echocardiography. Int J Cardiol. 1992;34:216–8.
111. Thwaites BK, Stamatos JM, Crowl FD, et al. Transesophageal echocardiographic diagnosis of intraaortic thrombus during coarctation repair. Anesthesiology. 1992;76:638–9.
112. Chatrath R, Hagler DJ. Improved imaging of aortic coarctation using an intracardiac probe for transesophageal echocardiography. Tex Heart Inst J. 2004;31:194–5.
113. Kinsara A, Chan KL. Noninvasive imaging modalities in coarctation of the aorta. Chest. 2004;126:1016–8.
114. Stern H, Erbel R, Schreiner G, et al. Coarctation of the aorta: quantitative analysis by transesophageal echocardiography. Echocardiography. 1987;4:387–95.
115. Gopal AS, Arora NS, Vardanian S, et al. Utility of transesophageal echocardiography for the characterization of cardiovascular anomalies associated with Turner's syndrome. J Am Soc Echocardiogr. 2001;14:60–2.
116. Rudolph AM, Heymann MA, Spitznas U. Hemodynamic considerations in the development of narrowing of the aorta. Am J Cardiol. 1972;30:514–25.
117. Loffredo CA, Ferencz C, Wilson PD, et al. Interrupted aortic arch: an epidemiologic study. Teratology. 2000;61:368–75.
118. Celoria GC, Patton RB. Congenital absence of the aortic arch. Am Heart J. 1959;58:407–13.
119. Powell CB, Stone FM, Atkins DL, et al. Operative mortality and frequency of coexistent anomalies in interruption of the aortic arch. Am J Cardiol. 1997;79:1147–8.
120. Ramaswamy P, Lytrivi ID, Thanjan MT, et al. Frequency of aberrant subclavian artery, arch laterality, and associated intracardiac anomalies detected by echocardiography. Am J Cardiol. 2008;101:677–82.
121. Schreiber C, Eicken A, Vogt M, et al. Repair of interrupted aortic arch: results after more than 20 years. Ann Thorac Surg. 2000;70:1896–9; discussion 1899–900.
122. Tchervenkov CI, Jacobs JP, Sharma K, et al. Interrupted aortic arch: surgical decision making. Semin Thorac Cardiovasc Surg Pediatr Card Surg Annu. 2005:92–102.
123. Flint JD, Gentles TL, MacCormick J, et al. Outcomes using predominantly single-stage approach to interrupted aortic arch and associated defects. Ann Thorac Surg. 2010;89:564–9.
124. Dillman JR, Yarram SG, D'Amico AR, et al. Interrupted aortic arch: spectrum of MRI findings. AJR Am J Roentgenol. 2008;190:1467–74.
125. Geva T, Hornberger LK, Sanders SP, et al. Echocardiographic predictors of left ventricular outflow tract obstruction after repair of interrupted aortic arch. J Am Coll Cardiol. 1993;22:1953–60.
126. Jacobs ML, Rychik J, Murphy JD, et al. Results of Norwood's operation for lesions other than hypoplastic left heart syndrome. J Thorac Cardiovasc Surg. 1995;110:1555–61; discussion 1561–2.
127. Rychik J, Murdison KA, Chin AJ, et al. Surgical management of severe aortic outflow obstruction in lesions other than the hypoplastic left heart syndrome: use of a pulmonary artery to aorta anastomosis. J Am Coll Cardiol. 1991;18:809–16.
128. Apfel HD, Levenbraun J, Quaegebeur JM, et al. Usefulness of preoperative echocardiography in predicting left ventricular outflow obstruction after primary repair of interrupted aortic arch with ventricular septal defect. Am J Cardiol. 1998;82:470–3.
129. Russell HM, Forsberg K, Backer CL, et al. Outcomes of radial incision of the tricuspid valve for ventricular septal defect closure. Ann Thorac Surg. 2011;92:685–90; discussion 690.
130. Hillman HD, Mavroudis C, Backer CL. Patent ductus ateriousus. In: Mavroudis C, Backer CL, editors. Pediatric cardiac surgery. 3rd ed. Philadelphia: Mosby; 2003. p. 223–33.
131. Russell IA, Rouine-Rapp K, Stratmann G, Miller-Hance WC. Congenital heart disease in the adult: a review with internet-accessible transesophageal echocardiographic images. Anesth Analg. 2006;102(3):694–723.

132. Cahalan MK. Intraoperative transesophageal echocardiography: an interactive text and atlas. New York: Churchill Livingstone Interactive Publication; 1996.
133. Gaynor WJ. Aortopulmonary window and aortic origin of a pulmonary artery. In: Mavroudis C, Backer CL, editors. Pediatric cardiac surgery. 3rd ed. Philadelphia: Mosby; 2003. p. 353–60.
134. Backer CL, Mavroudis C. Vascular rings and pulmonary artery sling. In: Mavroudis C, Backer CL, editors. Pediatric cardiac surgery. 3rd ed. Philadelphia: Mosby; 2003. p. 234–50.
135. Backer CL, Mavroudis C. Coarctation of the aorta. In: Mavroudis C, Backer CL, editors. Pediatric cardiac surgery. 3rd ed. Philadelphia: Mosby; 2003. p. 251–72.
136. Jonas RA. Interrupted aortic arch. In: Mavroudis C, Backer CL, editors. Pediatric cardiac surgery. 3rd ed. Philadelphia: Mosby; 2003. p. 273–82.